ANTHROPOLOGY

Indirect genetic effects among neighbors promote cooperation and accelerate adaptation in a small-scale human society

Jordan S. Martin[1,2]*, Bret Beheim[3], Michael Gurven[4], Hillard Kaplan[5], Jonathan Stieglitz[6], Benjamin C. Trumble[7], Paul Hooper[8], Dan Cummings[5], Daniel Eid Rodriguez[9], Adrian V. Jaeggi[1]

Explaining the rapid evolution of human cooperation and its role in our species' biodemographic success remains a major evolutionary puzzle. To address this challenge, we tested a social drive hypothesis, which predicts that social plasticity and social selection in human groups cause indirect genetic effects that accelerate the adaptation of fitness, promoting population growth via feedback between the environmental causes and evolutionary consequences of cooperation. Using Bayesian multilevel models to analyze fertility data from a small-scale society, we demonstrate that density- and frequency-dependent indirect genetic effects on fitness promote the evolution of cooperation among neighboring women, increasing the rate of contemporary adaptation by ~5×. Our results show how interactions between the genetic and socioecological processes shaping cooperation in reproduction can drive rapid growth and social evolution in human populations.

INTRODUCTION

Humans tend to live in groups with relatively low average genetic relatedness (*1*), reproductive skew (*2*), and genetic diversity (*3*), conditions which are expected to inhibit the pace of and potential for social evolution (*4*). Nevertheless, our species has evolved ecologically dominant social systems characterized by extensive cooperation and collective action (*5*) over the rapid scale of tens to hundreds of thousands of years (*6*), along with an exceptional capacity for population growth (*7*–*9*) and accelerated reproductive tempo in comparison to other primates (*10*, *11*). Human societies also differ markedly in their childcare practices (*12*), food sharing norms (*13*, *14*), modes of wealth transmission (*15*, *16*), and various other forms of fitness interdependence (*17*), demonstrating considerable plasticity in response to the relative risks and affordances provided by the local environment (*18*). While mutually beneficial cooperation clearly predominates in human interactions outside of the family (*19*, *20*), the origins of humans' uniquely flexible and fast evolving social behavior remain difficult to explain using standard models from evolutionary biology and behavioral ecology (*21*, *22*). This has led to a disconnect between evolutionary research on cooperation in humans and other animals (*23*, *24*). Developing generalizable models of humans' rapid social evolution thus remains an essential challenge for further expanding and integrating evolutionary theory across the biological and behavioral sciences.

Understanding interactions between social, ecological, and evolutionary dynamics is also a fundamental issue for 21st century biology more generally (*25*), both for predicting how populations will respond to climate warming and other environmental changes (*26*–*28*), as well as for explaining unexpected patterns of contemporary adaptation (*29*, *30*). The potential for a population to evolve via natural selection is fundamentally determined by the amount of heritable genetic variation shaping individuals' fitness within a given environment (*31*). Therefore, quantifying heritable variation in fitness is essential for predicting the pace of adaptive evolution (*30*). However, genes and environments often interact in complex ways that defy simple predictions about population change. For humans and many other species, social interactions generate feedback between developmental and ecological processes, affecting both the selection pressures on organisms' phenotypes and the expression of heritable variation in fitness. This means that social interactions can also play a central role in determining the potential for a population to undergo adaptive microevolutionary change (*32*, *33*), also known as evolvability (*34*).

Social interactions influence evolvability by generating heritable associations between direct genetic effects (DGEs) on the phenotypes that determine an individual's fitness W and indirect genetic effects (IGEs) on the phenotypes that help or hinder the fitness of others W' in the social environment (Fig. 1A). For example, in flour beetles (*Tribolium castaneum*) and laying hens (*Gallus gallus*), alleles that promote cannibalistic behavior tend to increase individual productivity (a positive DGE on fitness) at the expense of decreased conspecific survival [a negative IGE on fitness; (*35*, *36*)]. Conversely, in female baboons (*Papio cynocephalus* and *Papio anubis*), alleles that promote giving grooming to others also promote receiving grooming from others, which is associated with increased survival [a positive IGE on fitness; (*37*)]. When such DGEs and IGEs on fitness components are heritable in a population, the magnitude of their covariance, denoted $\mathrm{cov}(\mathbf{W_D}, \mathbf{W_I})$, is expected to magnify or diminish the evolvability of fitness, $e_{W|\bar{r}}$, modulated by the average relatedness $\bar{r}$ among social partners (Fig. 1A and Eq. 17). This occurs because alleles influencing individual fitness will, on average, also be associated with positive or negative effects on fitness from interactions with others. As shown in Fig. 1B, IGEs can thus accelerate

[1]Human Ecology Group, Institute of Evolutionary Medicine, University of Zurich, Zurich, Switzerland. [2]Department of Fish Ecology and Evolution, EAWAG, Kastanienbaum, Switzerland. [3]Department for Human Behavior, Ecology and Culture, Max Planck Institute for Evolutionary Anthropology, Leipzig, Germany. [4]Department of Anthropology, University of California Santa Barbara, Santa Barbara, CA, USA. [5]Economic Sciences Institute, Chapman University, Orange, CA, USA. [6]Institute of Advanced Study Toulouse, University of Toulouse, Toulouse, France. [7]School for Human Evolution and Social Change and Center for Evolution and Medicine, Institute of Human Origins, Arizona State University, Tempe, AZ, USA. [8]Department of Anthropology, University of New Mexico, Albuquerque, NM, USA. [9]Faculty of Medicine, Universidad Mayor de San Simon, Cochabamba, Bolivia.
*Corresponding author. Email: jordanscott.martin@eawag.ch

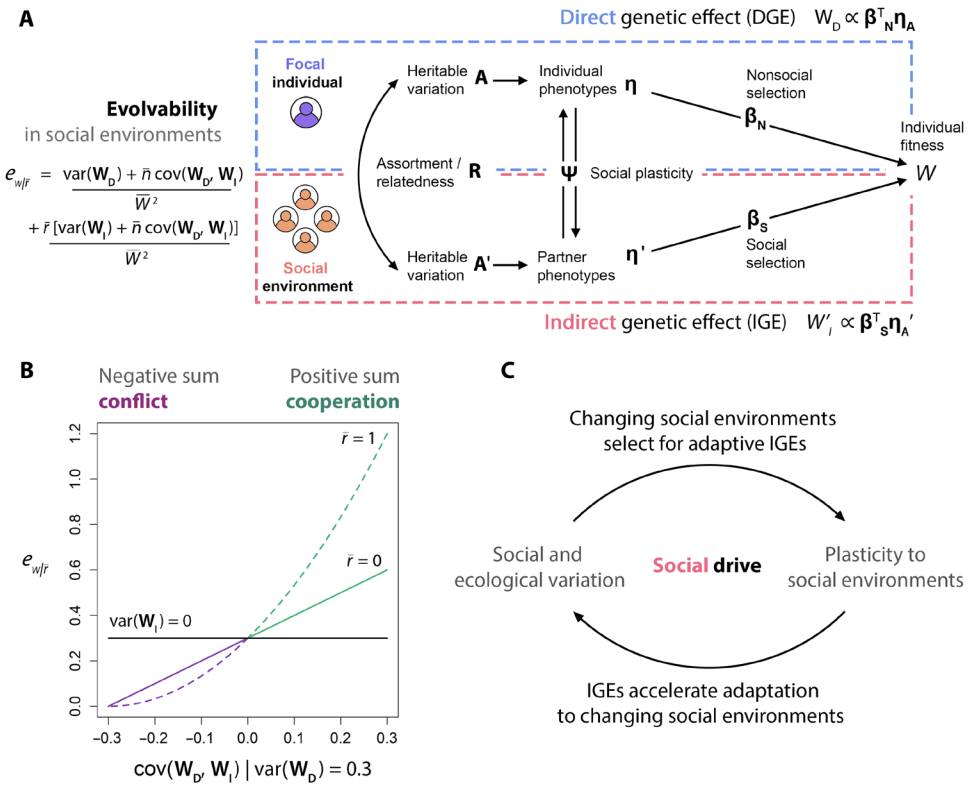

Fig. 1. IGEs and the adaptation of fitness in social environments. (**A**) The total DGE on an individual's fitness W is determined by and proportional to $\propto$ the total magnitude of nonsocial selection $\boldsymbol{\beta}_N$ acting on heritable variation $\mathbf{A}$ in all their fitness-relevant phenotypes $\boldsymbol{\eta}$; the total IGE on their fitness is in turn proportional to the total magnitude of social selection $\boldsymbol{\beta}_S$ acting on heritable variation $\mathbf{A}'$ in all fitness-relevant phenotypes $\boldsymbol{\eta}'$ expressed by cooperators or competitors in their environment. These heritable effects are shaped both by social plasticity $\boldsymbol{\Psi}$ and average assortment/relatedness $\mathbf{R}$ across phenotypes. See Table 1 for an overview of key notation and terminology. Evolvability (potential for adaptation) of fitness in social environments $e_{W|\bar{r}}$ is in turn determined by the total variances of IGEs and DGEs among individuals in the population (which are always positive), the sign and magnitude of covariance between individuals' DGEs and IGEs scaled by the expected number of social partners $\bar{n}$, and the average relatedness $\bar{r}$ between individuals and their social partners [expanding Fisher's fundamental theorem; (*31*, *40*)]. Note that $100 * e_{W|\bar{r}}$ can be interpreted as the expected % change in fitness attributable to natural selection, which reflects adaptive change in the instantaneous growth rate of the population. See Eqs. 3 to 18 for mathematical details. (**B**) Given a fixed level of DGEs, here $\text{var}(\mathbf{W_D}) = 0.3$ with $\overline{W} = 1$ and $\bar{n} = 1$, the covariance of DGEs and IGEs $\text{cov}(\mathbf{W_D}, \mathbf{W_I})$ can accelerate or inhibit the expected rate of change in the heritable component of average population fitness [i.e., adaptation; (*41*)]. (**C**) Conceptual overview of the social drive hypothesis of rapid human adaptation that is tested empirically in this paper.

or constrain adaptation (the genetic evolution of individual fitness) in social environments, even in the absence of assortment and relatedness (*33*, *38*–*41*).

The magnitude of IGEs on fitness is influenced both by selection due to others' phenotypes (social selection $\boldsymbol{\beta}_S$) and plasticity toward others' phenotypes (social plasticity $\boldsymbol{\Psi}$) [Fig. 1A and (*33*, *38*); see Table 1 for an overview of key notation and terminology]. This is because social plasticity changes the amount of heritable variation expressed in the fitness-relevant phenotypes of individuals and their social partners, while social selection causes this heritable variation among social partners to become associated with variation in individual fitness (Fig. 1A and Eqs. 2 to 8). As a consequence, $\text{cov}(\mathbf{W_D}, \mathbf{W_I})$ not only determines the evolvability of fitness but also provides a direct, operational measure of whether selection from the social environment is acting to promote cooperation $\text{cov}(\mathbf{W_D}, \mathbf{W_I}) > 0$ (i.e., positive-sum payoffs among social partners) or conflict $\text{cov}(\mathbf{W_D}, \mathbf{W_I}) < 0$ (i.e., zero-sum payoffs) across fitness-relevant phenotypes (Fig. 1B and Eqs. 11 to 12). By accounting for gene-by-social environment interactions, due to both social plasticity and fluctuating social selection on fitness, $\text{cov}(\mathbf{W_D}, \mathbf{W_I})$ can also vary across contexts that differentially shape the expression of social strategies. The quantitative genetic covariance $\text{cov}(\mathbf{W_D}, \mathbf{W_I})$ is thus an extremely useful evolutionary parameter, which can directly test predictions about the adaptive evolution of plastic traits in heterogeneous social environments. However, despite extensive experimental work [e.g., (*42*–*44*)], few empirical studies have investigated IGEs and their covarying effects on fitness components outside of laboratory or agricultural settings [(*45*); see e.g., (*46*–*50*) for notable exceptions], limiting our understanding of how ecological processes may feedback with adaptive social evolution in humans and other animals.

Here, we synthesize these evolutionary genetic and anthropological perspectives to test the hypothesis that socio-eco-evolutionary feedback is central to explaining rapid adaptation in human societies. Given the extensive plasticity of human social systems and reproductive traits (*51*, *52*), it is not unexpected that heritable effects on fitness components such as fertility are often caused by ubiquitous but poorly understood gene-by-environment interactions (*53*). Human societies occupying heterogeneous environments thus provide a powerful but underappreciated opportunity to investigate the

Table 1. Formal notation and terminology. Symbols are used throughout the manuscript to refer to focal individuals as well as individuals in their social environment ("social partners"), the latter being denoted by a prime symbol. See Figs. 1 and 3 for visualizations of the mathematical relationships among these quantities.

Term	Symbol	Verbal definition	Key equations
Individual fitness	W	The expected number of offspring produced by an individual over a time period (*96*)	Eqs. 1A and 3
DGE	W_D	The additive effect of an individual's alleles on their own fitness	Eqs. 2 and 7
IGE	W_I	The additive effect of an individual's alleles on the fitness of social partners	Eqs. 2 and 7 to 9
DGE-IGE covariance	$\mathrm{cov}(\mathbf{W_D}, \mathbf{W_I})$	The population-level covariance between individuals' fitness DGEs and IGEs	Eqs. 2, 12, and 13
Evolvability	$e_{W\|\bar{r}}$	The potential for adaptive evolution of individual fitness, which is contingent on average relatedness among social partners	Eqs. 18 to 21
Fitness-relevant phenotypes	$\boldsymbol{\eta}$	Complex traits causing variation in individual fitness	Eqs. 3 to 15
Social plasticity	$\boldsymbol{\Psi}$	Changes in phenotypes caused by the expression of phenotypes in social partners	Eq. 5
Nonsocial and social selection on fitness-relevant phenotypes	$\boldsymbol{\beta_N}, \boldsymbol{\beta_S}$	The respective contribution of individual and social partner phenotypes to differential fitness among individuals	Eqs. 3, 4, and 6 to 14
Social selection on heritable fitness variation (social fitness slope)	β_{SW}	Change in individual fitness as a function of the fitness DGE of social partners, quantifying the total heritable effects of social selection on and plasticity in fitness-relevant phenotypes	Eqs. 2, 12, and 13
Density dependence	β_D	Change in the social fitness slope due to the number of social partners	Eq. 1E
Frequency dependence	β_I, β_{Ir}	Change in the social fitness slope due to the interaction between the fitness DGE of individuals and their social partners, as well as their relatedness	Eq. 1E

consequences of IGEs for the evolvability of social behavior and fitness (*54*). We propose a general explanatory model of human adaptation emphasizing feedback between fluctuating social selection, which maintains adaptive social plasticity in cooperation (*55*), and the developmental effects of social plasticity and cooperation on the evolvability of fitness $e_{W|\bar{r}}$ via IGEs (Fig. 1C). Building on recent work investigating the role of IGEs in rapid evolution (*56*), we refer to this as the social drive hypothesis of human adaptation.

On the basis of formal theory of IGEs (*33*, *41*), we expect that positive social selection on ($\boldsymbol{\beta_S} > 0$) and social plasticity in ($\boldsymbol{\Psi} > 0$) fitness-relevant phenotypes will generate $\mathrm{cov}(\mathbf{W_D}, \mathbf{W_I}) > 0$ on fitness components such as fertility, enhancing $e_{W|\bar{r}}$ and thus accelerating adaptation of a population (Fig. 1B). If selection for cooperation or conflict in reproduction had remained relatively constant throughout humans' evolutionary history, plasticity in reproductive behavior may not have evolved (*57*). However, selection pressures on social interactions are likely to fluctuate due to environmental variation as well as density and frequency dependence in human societies (*54*), sustaining selection for adaptive plasticity in cooperation and in turn maintaining the amplifying effects of IGEs on evolutionary change across generations (*55*). These eco-to-evo and evo-to-eco effects (*25*) create the joint conditions for sustained feedback between plastic social interactions, social environmental change, and evolvability across time, which we refer to as social drive (Fig. 1C).

To test our social drive hypothesis, we developed a Bayesian IGE model (*58*) for investigating the evolutionary quantitative genetics of cooperation in reproduction across heterogeneous social environments (Materials and Methods). We applied this model to a rare, multidecade database of natural fertility variation among the Indigenous Tsimane people of lowland Bolivia (Fig. 2), who have participated for over two decades in generating extensive genealogical, socioecological, and demographic data about their society as part of

Fig. 2. The Tsimane people of Bolivia. The Tsimane are an Indigenous people that occupy a broad territory within and surrounding the lowland Amazonian forests of Bolivia, who largely rely on foraging, hunting, and horticulture for their subsistence (*59*). Multiple Tsimane families tend to live in close spatial proximity together, forming clusters or "neighborhoods," and cooperate in daily resource production, childcare, manual labor, and other fitness-relevant activities. These neighborhoods are nested within broader communities. (**A**) Neighboring kin socializing together, with a grandmother sitting in contact with her daughters and grooming her granddaughter. (**B**) Children from two neighboring households play together while their mothers prepare a shared meal. (**C**) Many families gather for a community-wide educational event. (**D**) Local ecological conditions can vary appreciably across the Tsimane territory, from forests to open grasslands and riverine habitats. (**E**) For the 93 communities included in our fertility dataset (see Materials and Methods), those lacking information on reproductively active neighbors are filled orange, while those with neighbor information are filled yellow. The radiuses of yellow circles are scaled by the total number of reproductively active neighbors meeting our selection criteria that contributed to the dataset, ranging from 2 to 83 women per community (median = 8, mean = 14). Photo credit: Jordan Scott Martin. All photographs were taken and used for scientific publication with community and family consent.

the ongoing Tsimane Health and Life History Project (THLHP) [see (*59*) for a detailed overview]. To our knowledge, this is the largest demographic dataset available on any contemporary subsistence-oriented society. The Tsimane primarily rely on foraging and horticulture, with families tending to live in spatially clustered "neighborhoods" composed of interdependent households who engage in extensive trade and collective action in resource production (*60*). We expect that individuals' interdependence with their neighbors is likely to vary in response to factors such as their kinship and the density and productivity of local households, providing scope for fluctuating selection on reproductive behavior and social interactions across space and time. Moreover, as a consequence of exogamy and migration among communities, average pairwise relatedness among reproductive women in neighboring households (sample $\bar{r} = 0.16$) and communities (sample $\bar{r} = 0.04$) tends to be relatively modest, and overlap between matrices of genetic relatedness and community and neighborhood of residence was low across our sample (adjusted RV coefficients = 0.03 to 0.10), allowing us to differentiate genetic, social, and environmental effects on fitness across the population.

We analyzed data on 6218 recorded births from 1669 women across 93 Tsimane communities. We used fertility data to proxy variation in women's fitness because mortality risk among both reproductive adults and their offspring has been persistently declining across the Tsimane population in recent decades and was relatively low throughout the study period (expected annual probability < 0.04 for children 0 to 4 years of age and adults < 70 years of age; fig. S1). Rather than using lifetime fertility measures, we only analyzed data on births that could be localized to the year and community in which they took place, covering an average of 3.5 births over 9.2 years of a woman's reproductive career (see Supplementary Text for comparison to other demographic approaches). For a subset of individuals ($N = 501/57$ communities), information was also available on the identity of neighboring, reproductively active women living within 50 m of their household during the recorded births (mean neighbors $n = 2.4$), which we used to estimate IGEs on fertility. Adjusted for environmental variation in fertility due to age, birth year, residual correlations among neighbors, spatial variation among communities, spousal/father identity, and maternal effects (as a proxy of common childhood environments), our Bayesian multilevel model estimated the magnitude of variation in DGEs $\mathrm{var}(\mathbf{W_D})$, IGEs $\mathrm{var}(\mathbf{W_I})$, and their covariance $\mathrm{cov}(\mathbf{W_D}, \mathbf{W_I})$ on fertility among neighboring women. This was accomplished by treating fertility as a social reaction norm (*54*, *58*), with the covariance among women's DGEs and IGEs on fertility estimated using a slope parameter β_{SW} describing how a focal woman's fertility rate was expected to change in response to the mean fertility DGE of her neighbors (Fig. 3A; see Materials and Methods). To account for potential sources of

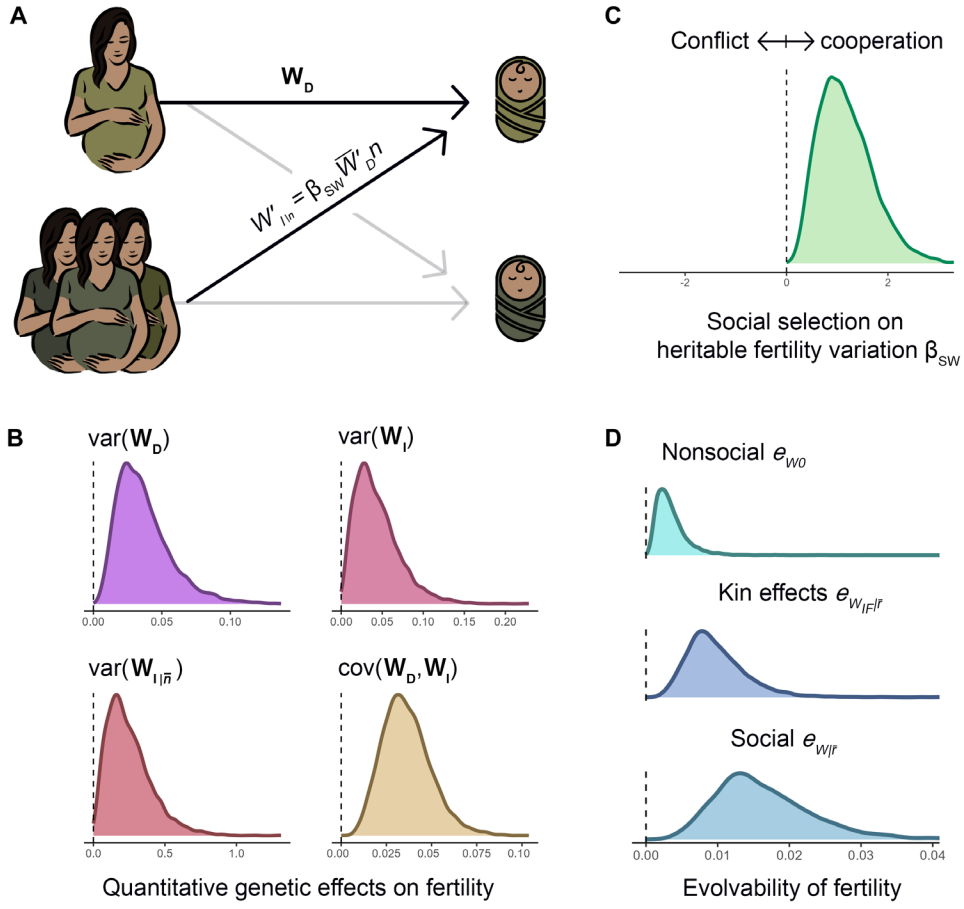

Fig. 3. Social selection, IGEs, and the evolvability of Tsimane fertility. (**A**) Conceptual overview of our Bayesian multilevel IGE model [Eqs. 1A to 1C; based on (*58*)]. IGEs were estimated using the slope β_{SW} of a focal woman's fertility on the mean DGE of her neighbors $\overline{W'}_D$ scaled by the total number of neighbors n, such that $\text{var}(\mathbf{W}_{\mathbf{I}|\bar{n}}) = \text{var}(\mathbf{W}_{\mathbf{D}})\beta_{SW}^2\bar{n}^2$ and $\text{cov}(\mathbf{W}_{\mathbf{D}}, \mathbf{W}_{\mathbf{I}}) = \text{var}(\mathbf{W}_{\mathbf{D}})\beta_{SW}$ (Eq. 2), where the slope on W_D is fixed to 1 by construction (see Materials and Methods for mathematical details). (**B**) Posterior distributions for average quantitative genetic effects on fertility, shown both for the variance in marginal IGEs due to the average effect on a single neighbor ($n = 1$) and the total IGEs due to the average number of neighbors in the sample ($\bar{n} = 2.4$). (**C**) Posterior distribution of the average β_{SW} among Tsimane women, where $\beta_{SW} > 0 \equiv \text{cov}(\mathbf{W}_{\mathbf{D}}, \mathbf{W}_{\mathbf{I}}) > 0$ indicates net selection on heritable fertility variation for cooperation among neighbors (positive-sum payoffs), while $\beta_{SW} < 0 \equiv \text{cov}(\mathbf{W}_{\mathbf{D}}, \mathbf{W}_{\mathbf{I}}) < 0$ indicates net selection for conflict (zero-sum payoffs). (**D**) Posterior distributions for the expected evolvability of fertility due to selection on heritable fertility variation among Tsimane women. The nonsocial evolvability e_{W0} ignores the evolutionary consequences of IGEs, the inclusive fitness evolvability $e_{W_{IF}|\bar{r}}$ only accounts for IGEs among kin ($\bar{r} = 0.16$), while the social evolvability $e_{W|\bar{r}}$ accounts for IGEs among all neighbors.

fluctuating social selection and gene-by-social environment interactions, the slope of a focal woman's fertility on the average DGE of her neighbors was also allowed to vary as a function of stochastic socioecological variation across communities, her neighborhood size β_D to account for density-dependent effects, and the interaction among her and her neighbors' DGEs β_I contingent on their average degree of relatedness β_{Ir}, providing a measure of positive (synergistic) or negative (antagonistic) frequency dependence (*54*) among kin and nonkin. On the basis of the social drive hypothesis, we tested three a priori predictions:

(i) On average in the population, a positive genetic covariance $\text{cov}(\mathbf{W}_{\mathbf{D}}, \mathbf{W}_{\mathbf{I}}) > 0$ will be observed between DGEs and IGEs on Tsimane women's fertility, due to social selection for and plasticity in cooperation among neighbors.

(ii) The evolvability of fitness $e_{W|\bar{r}}$, as proxied by heritable variation in women's fertility, will be substantially magnified by IGEs among both kin and non-kin, in comparison to the effects of DGEs alone.

(iii) Differences will occur in $\text{cov}(\mathbf{W}_{\mathbf{D}}, \mathbf{W}_{\mathbf{I}})$ across communities and neighborhoods, due to fluctuating social selection for and plasticity in cooperation.

RESULTS

Heritable fertility variation among neighbors

We quantitatively summarized estimates from our Bayesian model using posterior medians, 90% Bayesian credible intervals (CIs), and posterior probabilities of directional effects (positive/negative: p_+ / p_-), which provide a continuous, quantitative measure of support for our predictions. On average, after adjusting for environmental effects (fig. S2) and IGEs from neighbors, we found that DGEs on fertility were very small, $\text{var}(\mathbf{W}_{\mathbf{D}}) = 0.03$ (90% CI = [0.01, 0.08]) and $h^2 = 0.04$ (90% CI = [0.01, 0.08]). The heritability unadjusted for neighbor and spousal effects was approximately twice as large, $h^2 = 0.08$ (90% CI = [0.03, 0.14]), indicating that social effects make a sizeable contribution to the estimated genetic variance of

fertility. Overall, greater variance in fertility was due to total IGEs from neighbors, total $\mathrm{var}\left(\mathbf{W}_{\mathbf{I}|\overline{n}}\right) = 0.22$ (90% CI = [0.06, 0.56]) with marginal IGEs being of similar magnitude to DGEs, $\mathrm{var}\left(\mathbf{W}_{\mathbf{I}}\right) = 0.04$ (90% CI = [0.01, 0.10]) (Fig. 3B). This indicates that heritable variation in women's fertility tended to be explained more by indirect effects from genetic variation among their neighbors than direct effects from their own genetic inheritance, $\mathrm{var}\left(\mathbf{W}_{\mathbf{I}|\overline{n}}\right) - \mathrm{var}\left(\mathbf{W}_{\mathbf{D}}\right) = 0.19$ (90% CI = [0.01, 0.52], $p_+ = 0.96$). Moreover, we also found a positive genetic covariance between women's DGEs and their marginal IGE on the fertility of an average neighbor (Fig. 3B), $\mathrm{cov}\left(\mathbf{W}_{\mathbf{D}}, \mathbf{W}_{\mathbf{I}}\right) = 0.03$ (90% CI = [0.02, 0.06], $p_+ = 1.00$), providing support for prediction (i). This indicates that women who had a heritable tendency toward relatively higher fertility tended to also increase the fertility of neighboring women. During the observational period, the net effect of social plasticity and social selection on heritable fertility variation was thus acting to promote cooperation among neighbors, $\beta_{SW} = 1.10$ (90% CI = [0.43, 2.15], $p_+ = 1.00$) (Fig. 3C).

Social interactions enhance evolvability

From a quantitative genetic perspective, DGEs on fitness components such as fertility summarize the total magnitude of nonsocial selection acting on heritable variation in individual phenotypes (Eqs. 10 to 15). The small magnitude of DGEs thus indicates that there was very weak individual selection acting on heritable fertility variation among the Tsimane, as reflected by the small nonsocial evolvability (i.e., assuming no IGEs; Eq. 21), $e_{W0} = 0.003$ (90% CI = [0.001, 0.007]). However, interactions among neighboring women appreciably enhanced the evolvability of fertility ($e_{W|\overline{r}} = 0.015$, 90% CI = [0.007, 0.030]; Fig. 3D), given the average number of ($\overline{n} = 2.4$) and relatedness ($\overline{r} = 0.16$) among neighboring, reproductively active women. In support of prediction (ii), plasticity in and selection for cooperation among neighbors thus acted to accelerate the adaptation of Tsimane fertility by a factor of $\frac{e_{W|\overline{r}}}{e_{W0}} = 5.18$ (90% CI = [2.38, 11.26], $p_+ = 0.99$). Only considering inclusive fitness effects among related women (Eqs. 19 to 20), IGEs are still expected to accelerate the evolvability of fertility by a factor of $\frac{e_{W_{IF}|\overline{r}}}{e_{W0}} = 2.97$ (90% CI = [1.51, 6.93]). This indicates that, over the average observation time of only 9 years per woman (approximately one-third of a woman's typical reproductive career), IGEs on fertility were expected to increase the quantitative genetic component of population fitness by ~1.5%, with direct effects only contributing ~0.3% of this change, comparable to median evolvabilities based on lifetime reproductive success in other animal and plant taxa (*61*).

Social and ecological variation generates fluctuating selection

In addition to these population average effects, the magnitude of plasticity in and social selection for cooperation in fertility varied considerably among communities and neighborhoods (Fig. 4), providing support for prediction (iii). Given that Tsimane women may move multiple times during their reproductive career, individuals are thus likely to experience fluctuating selection on their fertility and social interactions with neighbors across their life span. Community-level variation in the covariance of DGEs and IGEs was relatively large, $\mathrm{var}\left[\mathrm{cov}\left(\mathbf{W}_{\mathbf{D}}, \mathbf{W}_{\mathbf{I}}\right)\right] = 0.17$ (90% CI = [0.08, 029]) and $\mathrm{cov}\left(\mathbf{W}_{\mathbf{D}}, \mathbf{W}_{\mathbf{I}}\right)$ range = −0.08 to 0.22 (Fig. 4A). This indicates that local socioecological factors played an important role in structuring the magnitude of social plasticity and social selection for cooperation among neighbors. Neighborhood size tended to decrease women's marginal IGEs on the fertility of their neighbors

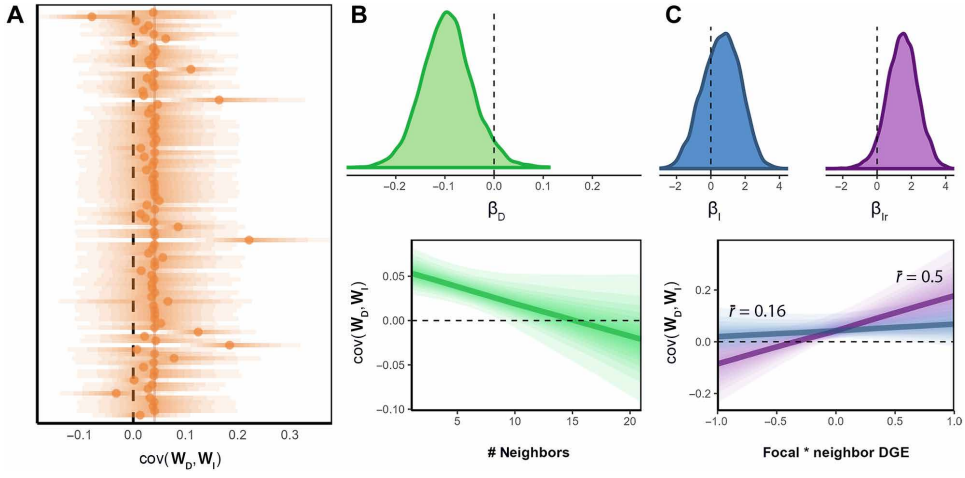

Fig. 4. Fluctuating social selection across Tsimane neighborhoods and communities. Posterior estimates for patterns of fluctuating social selection on heritable fertility variation β_{SW} and resulting community- and neighborhood-level variation in the quantitative genetic covariance $\mathrm{cov}\left(\mathbf{W}_{\mathbf{D}}, \mathbf{W}_{\mathbf{I}}\right)$ (Eqs. 1D and 1E). (**A**) Posterior medians (points) and 10 to 90% CIs (shaded lines) for community-specific (*y* axis) genetic covariances (*x* axis), with values at 0 indicating no net selection on heritable fertility variation and values below/above 0 indicating net selection for conflict/cooperation among neighbors within the community. Note that because of partial pooling of random effects, communities with fewer observed neighbors tend to cluster more around the average across communities (0.03, solid line). Therefore, the plotted predictions are likely to underestimate the true magnitude of variation among communities. (**B**) Posterior distributions (top) for density-dependent selection β_D and its resulting effect (bottom) on the magnitude of $\mathrm{cov}\left(\mathbf{W}_{\mathbf{D}}, \mathbf{W}_{\mathbf{I}}\right)$ across neighborhoods of varying size, with median predictions shown by the dark line and 10 to 90% Bayesian CIs indicated by the shaded bands. (**C**) The same is shown for frequency-dependent selection β_I (blue) and its moderation by neighbor relatedness β_{Ir} (purple), with predictions plotted as function of the interaction between women's fertility DGEs and the average fertility DGE of their neighbors. The increased slope in higher relatedness neighborhoods (shown for coresiding sisters, $\overline{r} = 0.5$) indicates synergy (positive frequency dependence) among kin.

($\beta_D = -0.10$, 90% CI = [−0.18, −0.01], $p_- = 0.96$), providing evidence for negative density dependence that reduces the evolvability-enhancing effects of social interactions in denser neighborhoods (Fig. 4B). Independent of neighborhood size, we also found that the mean DGE of a woman's neighbors tended to have a synergistic interaction with her own fertility DGE but only in neighborhoods of closely related women ($\beta_I = 0.65$, 90% CI = [−1.18, 2.33], $p_+ = 0.62$; median $\beta_{Ir} = 1.50$, 90% CI = [0.00, 2.95], $p_+ = 0.95$), providing support for positive frequency dependence among kin, acting to further accelerate or inhibit evolvability contingent on the expected composition of neighborhoods (Fig. 4C). This indicates that women with a heritable tendency toward higher fertility DGEs tended to have even greater realized fertility in neighborhoods of other related women with relatively high fertility DGEs. As women with higher DGEs were, on average, also found to have more positive IGEs on their neighbors, this result suggests that cooperation in fertility-promoting phenotypes is synergistic among related women living in close proximity, consistent with prior work demonstrating that kin-based cooperation is central to Tsimane sociality (*18*, *59*) and that division of labor, trade, and economies of scale enhance reciprocal returns among the most productive Tsimane households (*60*).

DISCUSSION

Overall, our results (Figs. 3 and 4) provide clear support for social drive as a critical eco-evolutionary process shaping the adaptation of human populations via IGEs. In both historic and contemporary human populations, fluctuating selection caused by density and frequency dependence, as well as rapid environmental change, has likely acted to promote and maintain adaptive social plasticity in fitness interdependence and cooperation among both related and unrelated group members, against the backdrop of sustained paternal and grandparental care that has also been crucial for human life history evolution (*7*, *8*, *13*, *18*). Thus, as humans have moved throughout the world and continuously transformed their environments, individuals have been able to flexibly shift their interactions with kin and nonkin group members, buffering themselves against ecological risk and social exploitation while also taking advantage of synergies arising from reciprocity, division of labor, economies of scale, and other mechanisms of mutually beneficial cooperation (*5*–*9*, *12*–*18*, *60*, *62*–*64*). As we observed among Tsimane women (Fig. 2), selection for cooperation in reproduction is expected to vary appreciably across neighborhoods in response to their size and composition, as well as across communities due to ecological differences (Fig. 4). This extensive variation in and sensitivity toward the social environment has in turn promoted cooperative or conflictual IGEs on fitness components such as fertility, acting to curtail or accelerate phenotypic adaptation and further change the composition of the social environment (Fig. 1, A and B). As a consequence, while other species lacking high relatedness and reproductive skew tend to exhibit small IGEs on fitness components (*45*), human populations such as the Tsimane often maintain a high degree of interdependence, with IGEs from group members having a much larger impact on the evolvability of individual fitness (Fig. 3). This dynamic feedback between socioecological and quantitative genetic processes within and across generations can sustain alignment between the direction of selection on and adaptive plasticity in the phenotype (Fig. 1C). Our social drive hypothesis thus provides an integrative explanation for the rapid pace of human social evolution as a consequence of IGEs generating socio-eco-evolutionary feedback.

Persistent developmental and contextual variation in inclusive fitness effects is expected to cause the adaptation of highly contingent social strategies, which allow individuals to plastically respond to the shifting costs and benefits of cooperation or conflict across social environments (*55*, *62*). An exciting avenue for future research will, therefore, be to uncover the specific behavioral and physiological mechanisms mediating IGEs on fertility, as well as other fitness components shaping the timing and tempo of human life history [e.g., age of first reproduction; (*47*)], further promoting the synthesis of evolutionary anthropological and quantitative genetic perspectives on human sociality (*54*). In this sense, the social drive hypothesis provides a general functional explanation for rapid adaptation that is complementary with a broad class of proximate models emphasizing the importance of cognitive and developmental mechanisms facilitating intra- and intergenerational plasticity in human phenotypes, such as language and sociocultural learning (*7*), as well as specific cultural evolutionary models, such as the institutional paths hypothesis (*64*), that emphasize self-interested individuals' ongoing negotiation of normative interactions via plasticity and selection within cultural groups.

Regardless of the specific mechanisms involved, it is clear that our species is unique in its reliance on complex forms of cognitively and culturally mediated social interaction (*5*, *7*, *21*, *22*) and that understanding the dynamics of these interactions is crucial for explaining otherwise puzzling patterns of growth, as well as decline, in human populations. As we demonstrate here, quantitative genetic theory provides a flexible framework for understanding how human social interactions influence phenotypic adaptation via sustained covariance between DGEs and IGEs on fitness (*39*–*41*). The causal networks sustaining social drive within human societies can thus be seen as one of a variety of potential mechanistic pathways through which accelerated quantitative genetic change can occur in socially plastic traits (*54*–*56*). Our findings demonstrate that this radical potential for socio-eco-evolutionary feedback is crucial for explaining our species' capacity, documented throughout our evolutionary history and across the world today, for exceptional population growth and rapid adaptation via intra- and interfamilial cooperation (*6*–*9*).

MATERIALS AND METHODS

Materials

Ethics statement

Informed consent was collected at three levels: by the individual, by the community, and by the Tsimane Gran Consejo (Tsimane governing body). All study protocols were approved by the Institutional Review Boards of the University of New Mexico (#07-157), the University of California Santa Barbara (#3-21-0652), and the Universiad San Simon, Cochabamba, Bolivia.

Fertility database

We compiled our fertility database from an extensive birth registry capturing 9774 births from 2540 women recorded by the THLHP, spanning a 20-year period from the beginning of the THLHP in 2002 to 2022. See (*59*) for an extensive overview of the Tsimane population and the THLHP. Our analyses required that we were able to localize a woman's measured fertility to the community in which these births took place, with at least two or more births recorded in a community to effectively offset analyses for the window of

sampling (year of first birth to year of last birth) and thus estimate social effects on fertility relative to the time elapsed. Moreover, we excluded data on women who lacked age information, for whom their position in the population pedigree could not be resolved (e.g., due to missing information on parents), as well as from four communities lacking data for analyzing spatial effects. We compiled our fertility database from this subset of the total population registry, resulting in 6218 recorded births from 1669 women. On average, the remaining births were recorded from an average of 9.16 years of a woman's reproductive career within a given community, with a mean fertility of 3.51 births during this period. As shown in Fig. 2, our total dataset contained information on women's fertility across 93 Tsimane communities, of which 57 communities also contributed information about neighboring reproductively active women.

We further coordinated this subset of the birth registry with community information in the THLHP database to include various environmental measures of interest in the fertility database, which we adjusted for to reduce bias in estimates of additive genetic variation among women. GPS coordinates from each community center were used to capture spatial effects on fertility due to ecological variation across communities. A woman's age was calculated by the difference in years from her recorded birth in the registry to the onset of her community-specific reproductive window as recorded in the fertility database. The identity of a focal woman's mother was recorded to estimate maternal effects on her fertility (*65*), effectively proxying common environmental effects among sisters that may arise from sharing a birth mother and childhood home. Many older women ($N = 169$) did not have mothers listed in the birth registry and so were grouped together in an "unknown" category to offset for any bias due to mean differences among women with and without known mothers (e.g., due to temporal effects). The identity of the father for each of a woman's recorded births in a community was also recorded to adjust for the influence of spouses on their reproductive output (see below for discussion of potential bias due to extra-pair paternity). Tsimane fathers play an important role in shaping the productivity of their wives and households (*66*, *67*), and prior IGE research in other human populations has shown the importance of fathers in generating indirect effects on their spouse's reproduction (*47*, *48*). Some women had multiple birth fathers recorded during their period (e.g., due to separation, death, or other factors), and so we accounted for the additive effect of all fathers recorded during their reproductive period in a given community. Only five women in the dataset were missing information on the birth father.

Pedigree for estimating genetic effects

We developed a pedigree for our quantitative genetic analysis using data on parentage from the THLHP population census, which is based on genealogical data dating back over a century that has been developed through extensive family interviews within and across communities. Whenever using such a "social" pedigree (i.e., one not based on molecular markers), there is a risk that recorded and actual parentage will differ, introducing noise in the analysis. While this is an intrinsic limitation of our analysis, extensive prior work on comparable small-scale, nonindustrialized human societies with high rates of monogamy has indicated that rates of extra-pair paternity are in general quite low [~1% in both contemporary and historic human populations; (*68*)], suggesting that misassigned paternity is unlikely to have meaningfully biased population-level estimates from our models (*69*). We used the R package MCMCglmm (*70*) to convert our pedigree into an **A** matrix capturing the expected, standardized relatedness coefficients among all women in our fertility database.

While observed similarity among relatives can also reflect pathways of cultural transmission, our analyses account for the full **A** matrix during estimation (see below), rather than relying on parent-offspring regression or other methods for which quantitative genetic estimates are more easily biased by shared environments among kin and nongenetic pathways of vertical transmission (*65*). Thus, we would only expect confounding of genetic effects if pathways of cultural inheritance during the study period were Mendelian and followed the same exponential decay across kin as expected for genetic inheritance, irrespective of spatiotemporal proximity among family members. This is very unlikely given the lack of evidence for temporally stable cultural differences in social and reproductive behavior across Tsimane communities (*71*). Furthermore, Tsimane engage in ambilocal marriage practices, with both patrilocality and matrilocality observed across families (*72*). As a result of regular migration of women away from their natal community, matrices of genetic relatedness, community identity, and neighborhood identity are only very weakly correlated among the women in our fertility database. In particular, as reported above, using the adjusted RV coefficient (*73*), which is a matrix correlation ranging from 0 to 1 with values closer to 1 indicating redundant matrices, we find that spatial, social, and genetic effects are largely independent in our sample (RV: 0.03 to 0.10). Moreover, our statistical analyses directly adjusted for spatial variation among communities and correlated environmental effects within neighborhoods, further suggesting against putative bias in quantitative genetic estimates caused by unmeasured cultural or socioecological effects.

Neighborhood structure for IGEs

To estimate IGEs from outside the family on women's fertility, we needed a spatially and temporally localized measure of neighborhood structure, as previous ethnographic and quantitative work has demonstrated the centrality of local kin and nonkin neighbors for cooperative food production, childcare, resource trading, and division of labor among the Tsimane [see (*59*, *60*, *67*) and references therein]. Broader social clusters such as the community level are likely to confound IGEs caused by direct social interactions and fitness interdependence with various sources of spatiotemporal variation in the nonsocial environment, which may correlate among women within the same local habitat and cause spurious signals of covariance in fitness effects. We, therefore, developed a neighbor matrix for women who had GPS data available on the location of their home during their reproductive career within a given community. On the basis of local knowledge of the typical size of cooperative household clusters, we considered any reproductively active woman coresiding within 50 m of a focal woman during her recorded childbirth to be a potential source of IGEs on the focal woman's fertility via their social interactions. To directly estimate IGEs, it was also essential that neighbors were present in the pedigree as well as the fertility database. Such data on reproductively active neighbors were only available for a subset of women. Thus, we structured our statistical model (see below) to take full advantage of the pedigree and fertility information across all women in the sample while also estimating potential IGEs among those women who had spatially and temporally localized data on neighborhood structure.

Methods

Statistical analyses

We developed Bayesian multilevel IGE models to estimate quantitative genetic effects on Tsimane women's fertility and directly test the primary predictions (i) to (iii) of our social drive hypothesis. Our Bayesian models were based on the recently proposed social animal model (*58*), which extends the so-called animal model used for quantitative genetic inference in natural populations to measure continuous reaction norms and IGEs expressed in social environments. This model has been shown to have desirable statistical power for detecting modest effects at our sample size (*58*). We forgo explicit use of the term "social animal model" to avoid any undesirable connotations arising from application of this method to data on a marginalized human population. This modeling approach allowed for estimating multiple sources of variation in IGEs within a population, e.g., due to individual, neighborhood, or community differences, while also avoiding causes of measurement error such as endogeneity bias that have previously been shown to limit reaction norm-based approaches to IGE models [see (*58*, *74*) for detailed discussion]. Briefly, endogeneity bias arises from environmental effects that generate a spurious signal of repeatable, heritable effects on a phenotype from social interactions. The social animal model handles this issue by specifying the key slope of interest β_{SW} directly on latent genetic parameters in the model, which are partitioned from various sources of correlated environmental effects among neighbors, thus avoid endogeneity bias during estimation that would otherwise arise from use of phenotypic correlations.

We estimated all models in a fully Bayesian framework using Markov Chain Monte Carlo (MCMC) in the Stan probabilistic programming language (*75*), implemented in the R statistical environment (*76*) using the RStan (v2.35.0.9000) and CmdStanR packages [v0.8.1; (*77*)]. The basic structure of our IGE model predicted the absolute fertility W of woman j observed in neighborhood k of community c as a social reaction norm

$$
\begin{gathered}
W_{jkc} = W_0 + e_{jkc} + W_{D_j} + \beta_{SW}\overline{W}'_{D_k} n_k + \phi\bar{\delta}_k + \epsilon_{jkc} \\
e_{jkc} = \beta_1 \text{years. observed}_j + \beta_2 \text{age}_j + \beta_3 \text{age}_j^2 + \beta_4 \text{missing. neighbors}_k + \\
\text{maternal. id}_j + \sum \text{father. id}_j + \sum \text{birth. years}_j + \text{community. id}_c \\
\text{if missing. neighbors}_k = 1, \text{then } \beta_{SW} = \phi = 0
\end{gathered}
\tag{1A}
$$

Note that fixed slopes are denoted with β, while random effects lack regression coefficients. Here, W_0 is the population intercept and e_{jkc} is the sum of individual j, neighborhood k, and community c environmental effects on the fertility measure. β_1 is an offset that adjusts the model to account for the fact that women differed in the total amount of time their fertility was recorded in the dataset. The variable years. observed_j was mean-centered and standardized so that genetic effects were estimated as deviations from W_0 with respect to the average reproductive window (9 years) across the sample. Age was also mean-centered and standardized to remove collinearity between the main and quadratic effects (*78*) and to condition predictions on the average age (26 years old). Random effects were included for the focal woman's mother maternal. id_j, for the sum of father/spousal effects $\sum \text{father. id}_j$ across all of the recorded fathers for her births (mean = 1.07, range: 0 to 4), for the sum of birth years $\sum \text{birth. years}_j$ for all years that a woman was recorded as being reproductively active in a given community, and for the spatial effect of her community community. id_c during the recorded births.

Adjusted for these environmental effects, the model estimated the focal woman's DGE on her observed fertility W_{D_j}. For women who had information available on reproductively active neighbors, the slope β_{SW} was also estimated for the focal woman's fertility on the mean DGE of her neighbors $\overline{W}'_{D_k}$, multiplied by her total number of neighbors n_k, which scaled β_{SW} to the marginal effect of a single average neighbor. To account for additional unmeasured environmental correlations between neighbors (e.g., microhabitat effects), which could generate a spurious relationships between neighbors' additive genetic values, the model also estimated coefficient ϕ capturing any nongenetic association between the fertility of the focal woman and the mean of her neighbors' fertility deviations $\bar{\delta}_k$, which were defined as the difference between their observed fertility measure and all other predicted effects on their fertility (i.e., a correlated residual environment effect). The residual ϵ_{jkc} captured any remaining unexplained variance in fertility independent of these combined effects. The term $\beta_4 \text{missing. neighbors}_k$ is an offset that accounted for any bias due to mean differences in fertility among women with and without information on neighbors, while the if else statement within the model likelihood accounted for the fact that variation due to β_{SW} and ϕ could only be estimated when neighbors were known.

All random effects in the model were assumed to be sampled from Gaussian distributions

$$
\begin{aligned}
\mathbf{W_D} &\sim N\left(0, \mathbf{A}\sigma_G\right) \\
\textbf{birth. year} &\sim N\left(0, \sigma_Y\right) \\
\textbf{maternal. id} &\sim N\left(0, \sigma_M\right) \\
\textbf{father. id} &\sim N\left(0, \sigma_F\right) \\
\textbf{community. id} &\sim N\left(0, \sigma_C\right) \\
\boldsymbol{\epsilon} &\sim N\left(0, \sigma_\epsilon\right)
\end{aligned}
\tag{1B}
$$

with a Gaussian Process function used to model spatial variation among communities such that

$$
\begin{aligned}
\textbf{community. id} &\sim \text{MVN}\left[\mathbf{0}, K(\mathbf{D} \mid \alpha, \rho)\right] \\
K(\mathbf{D} \mid \alpha, \rho) &= \alpha^2 \exp\left(-\frac{1}{2\rho^2}\mathbf{D}^2\right) + \mathbf{I}\sigma_\delta
\end{aligned}
\tag{1C}
$$

where $\mathbf{D}$ is a distance matrix among communities based on latitude and longitude, $K()$ is a double-exponential covariance kernel with marginal SD α and length scale ρ, and $\mathbf{I}$ is a diagonal identity matrix multiplied by a very small nonzero offset $\sigma_\delta = 1 \times 10^{-9}$ to ensure positive definiteness of the matrix (*79*, *80*). Generalized, weakly regularizing priors, $\beta \sim N(0, 1)$ and $\sigma, \alpha \sim$ exponential(2), and $\rho \sim$ inverse gamma(5, 5) were placed on all model parameters to enhance convergence and reduce the risk of false positives (*79*, *81*). Following (*58*), we estimated the additive genetic and residual SDs as transformed parameters $\sigma_G = \sqrt{\sigma_P^2 h^2}$ and $\sigma_\epsilon = \sqrt{\sigma_P^2(1-h^2)}$ from the total adjusted phenotypic SD σ_P, where $h^2 \sim beta(1.2, 1.2)$, to reduce posterior correlations among the scales of genetic and environmental effects that would otherwise result from our relatively

sparse relatedness matrix. Posterior distributions sampled from this model are summarized by median estimates, 90% Bayesian CIs, and posterior probabilities of directional effects (positive/negative: p_+ / p_-). We report 90% Bayesian CIs because they facilitate straightforward and intuitive interpretation, with a 90% CI excluding zero corresponding to a posterior probability ≥ 0.95 in support of the predicted directional effect (i.e., probability ≤ 0.05 against the prediction). More broadly, it should be noted that Bayesian inference is principally concerned with the entire posterior distribution, as the specific choice of CI is always semiarbitrary (*79*). This allows for focusing attention on continuous, quantitative measures of support for hypotheses, here expressed by p_+ / p_-, rather than on the binary designation of significant versus nonsignificant findings, thus reducing the risk of problems such as p-hacking (*82*).

As is typical for fertility, there was a strong right skew in the distribution of our raw data. To ensure that the observed neighbor effects were not simply a biased result of inappropriately applying a linear model, we also estimated a log-normal model that more effectively described the skewed distribution of fertility. With this model, we also found similarly strong evidence for the positive IGEs arising from neighbors as observed in the Gaussian model (median log scale $\beta_{SW} = 0.53$, 90% CI = [0.17, 1.20]). Therefore, we opted to use the simpler linear model without log transformation for all reported analyses, given the robustness of our central finding to the choice of distribution, the general robustness of quantitative genetic predictions to violations of normality (*83*), and the fact that our theoretical models and predictions (Fig. 1; see Eqs. 15 to 21 below) were much more easily and directly tested by assuming a Gaussian distribution, as additive versus multiplicative effects on the original data scale could be straightforwardly distinguished.

To quantify fluctuating social selection and changes in the covariance of direct and IGEs across neighborhoods and communities, we also expanded the basic model to allow for β_{SW} to vary as a function of other model parameters. In particular, we first estimated a multilevel model accounting for random differences in β_{SW} across communities, independent of mean differences in fertility across communities due to spatial effects

$$\boldsymbol{\beta}_{\mathbf{SW}} \sim \mathrm{N}\left(\beta_{\mathrm{SW}_0}, \sigma_{\beta c}\right) \tag{1D}$$

Here, β_{SW_0} is the fixed, average neighbor slope across communities. We then estimated a neighborhood-level model to more directly test for density- and frequency-dependent fluctuations in IGEs, which are expected to play a key role in maintaining social drive across generations (Fig. 1C). For a focal woman j in neighborhood k, the social reaction norm slope $\beta_{SW_{jk}}$ of her fertility on the additive genetic value of her neighbors $\overline{W}'_{D_k}$ was given by

$$\beta_{\mathrm{SW}_{jk}} = \beta_{\mathrm{SW}_0} + \beta_D\left(n_k - 1\right) + \left(\beta_I + \beta_{Ir}\bar{r}\right) W_{Dj} \tag{1E}$$

Density-dependent effects in response to the focal woman's number of neighbors n_k were estimated by β_D, where $n_k - 1$ was used to adjust the fixed slope β_{SW_0} to the expected value for a single neighbor ($n_k = 1$). These density-dependent effects may include dilution due to a reduced marginal impact of each neighbor on the fitness of the focal individual in larger groups (*74*), as well as shifting selection pressures for cooperation or conflict. We find that the sign of $\mathrm{cov}\left(\mathbf{W_D}, \mathbf{W_I}\right)$is predicted to change in the largest observed social groups (Fig. 4B), suggesting that both factors are likely contributing to the estimated magnitude and sign of β_D. The interactive effect β_I between the focal woman's DGE W_{D_j} and the DGE of neighbors provided an estimate of frequency dependence appropriate for continuous traits (*54*, *58*, *84*), indicating whether there is an additional multiplicative effect for synergy ($\beta_I > 0$) or antagonism ($\beta_I < 0$) among neighboring women. The coefficient β_{Ir} quantified how this frequency-dependent effect changed as a function of the average relatedness among neighbors $\bar{r}$, where $\bar{r}$ was mean-centered and standardized such that β_I could be interpreted as the expected level of frequency dependence in an average neighborhood ($\bar{r} = 0.16$). To reduce posterior correlations during sampling and aid model convergence, we centered the prior distributions for β_{SW_0} and h^2 on their corresponding posterior distributions estimated from the average effect model (Eqs. 1A to 1C).

Quantitative genetic parameters

By further processing MCMC estimates of the posterior distributions from Eqs. 1A to 1E, we were able to directly calculate population average (co)variances in DGEs and IGEs, as well as social and nonsocial evolvabilities (Figs. 1 and 3) while effectively carrying forward statistical uncertainty across stages of analysis (*85*, *86*). Following prior work by McGlothlin and Fisher (*41*), we calculated DGEs and IGEs for fertility such that

$$\begin{aligned}
\mathrm{var}\left(\mathbf{W_D}\right) &= \mathrm{var}\left(\mathbf{W_D}\right)\beta^2_{\mathrm{NW}} = \mathrm{var}\left(\mathbf{W_D}\right) \\
\mathrm{var}\left(\mathbf{W_I}\right) &= \mathrm{var}\left(\mathbf{W_D}\right)\beta^2_{\mathrm{SW}} \\
\mathrm{var}\left(\mathbf{W}_{\mathbf{I}|\bar{n}}\right) &= \mathrm{var}\left(\mathbf{W_D}\right)\beta^2_{\mathrm{SW}}\bar{n}^2 \\
\mathrm{cov}\left(\mathbf{W_D}, \mathbf{W_I}\right) &= \mathrm{var}\left(\mathbf{W_D}\right)\beta_{\mathrm{NW}}\beta_{\mathrm{SW}} = \mathrm{var}\left(\mathbf{W_D}\right)\beta_{\mathrm{SW}}
\end{aligned} \tag{2}$$

where β_{NW}, the total magnitude of nonsocial selection on fertility, is implicitly fixed to 1 because DGEs on fitness and its constitutive components are by definition maximally selected upon (*87*). Bold font is used here to distinguish population vectors from scalars. Note that $\beta_{SW} < 0$ and $\beta_{SW} > 0$ necessarily imply $\mathrm{cor}\left(\mathbf{W_D}, \mathbf{W_I}\right) = -1$ and $\mathrm{cor}\left(\mathbf{W_D}, \mathbf{W_I}\right) = 1$, respectively, due to symmetric effects among social partners (*74*). See also Eqs. 10 and 11 below.

These relationships demonstrate that the slope β_{SW} of focal fitness on partner fitness DGEs is proportional to the total magnitude of social selection acting across all fitness-relevant phenotypes. To see this, note that "fitness" is simply a composite trait reflecting the total effects on survival and reproduction caused by an organism's phenotypes within a given environment (*88*). In this sense, the heritable variation of a fitness component such as fertility is just the heritable variation across all phenotypes causing repeatable individual differences in fertility, i.e., experiencing selection via fertility. Therefore, following (*41*), fitness proxy W can be expressed as the product of nonsocial $\boldsymbol{\beta}_{\mathbf{N}}$ and social selection gradients $\boldsymbol{\beta}_{\mathbf{S}}$ on all individual $\boldsymbol{\eta}$ and social partner phenotypes $\boldsymbol{\eta}'$ affecting this fitness component

$$W_{jk} = W_0 + \overline{W}\left(\boldsymbol{\beta}^{\mathrm{T}}_{\mathbf{N}}\boldsymbol{\eta}_{\mathbf{j}} + \boldsymbol{\beta}^{\mathrm{T}}_{\mathbf{S}}\overline{\boldsymbol{\eta}_{\mathbf{k}}}' n_k\right) + \epsilon_{jk} \tag{3}$$

Selection gradients are unit mean-scaled relative to the average fitness $\overline{W}$ and T indicates transposition. The vectors $\boldsymbol{\eta}_{\mathbf{j}}$ and $\overline{\boldsymbol{\eta}_{\mathbf{k}}}'$ contain trait values of focal individual j and the mean of their social partners in group k, respectively, for all phenotypes affecting an

individual's relative fitness. Note that $\overline{\boldsymbol{\eta}_{\mathbf{k}}}' n_k = \boldsymbol{\eta}'_{\mathbf{k}} = \sum_i^{n_k} \eta'_i$ is the sum of indirect effects from each partner i in neighborhood k of size n. The stochastic residual effects ϵ are expressed as zero-centered deviations with respect to the global intercept W_0. An individual's total additive genetic value for fitness is then

$$W_{Aj} = \overline{W}\left(\boldsymbol{\beta}_{\mathbf{N}}^{\mathbf{T}}\boldsymbol{\eta}_{\mathbf{Aj}} + \boldsymbol{\beta}_{\mathbf{S}}^{\mathbf{T}}\boldsymbol{\eta}_{\mathbf{Aj}}\overline{n}\right) \tag{4}$$

where $\boldsymbol{\eta}_{\mathbf{Aj}}$ is a vector of total additive genetic values for all fitness-relevant phenotypes $\boldsymbol{\eta}$. The total additive genetic value for fitness represents an individual's heritable contribution to mean population fitness, incorporating the effects of social plasticity and relatedness across all fitness-relevant phenotypes (*41*). The exact quantitative relationship between social plasticity and the magnitude of the total additive genetic value will be contingent on the causal structure of interactions assumed for a given phenotype (*58*). Under the simple case of an instantaneous interaction with feedback (*38*), we expect that

$$\boldsymbol{\eta}_{\mathbf{Aj}} = (\mathbf{I} - \boldsymbol{\Psi}\boldsymbol{\Psi})^{-1}\left(\mathbf{a}_{\mathbf{j}} + \boldsymbol{\Psi}\mathbf{a}_{\mathbf{j}}\right) \tag{5}$$

where $\mathbf{a}_j$ is a vector of individual j's additive genetic values for all phenotypes before social interaction, $\mathbf{I}$ is an identity matrix, and $\boldsymbol{\Psi}$ is a matrix of interaction coefficients quantifying the magnitude of social plasticity among all fitness-relevant phenotypes $\boldsymbol{\eta}$. In general, we expect for social plasticity in humans' cooperative interactions, such as through reciprocal resource sharing and childcare ($\psi > 0$), to magnify standing additive genetic variance in the phenotype (*32*, *54*).

With this fitness model, the Robertson-Price identity (*89*, *90*) can be used to predict adaptation caused by selection on heritable fitness variation, ignoring changes generated by nonadaptive processes. In particular, the expected change in mean fitness, conditional on the current distribution of environmental states and marginal allelic effects in the population, is given by

$$\Delta\overline{W} = \frac{\mathrm{cov}\left[\overline{W}\left(\boldsymbol{\beta}_{\mathbf{N}}^{\mathbf{T}}\boldsymbol{\eta}_{\mathbf{A}} + \boldsymbol{\beta}_{\mathbf{S}}^{\mathbf{T}}\boldsymbol{\eta}_{\mathbf{A}}\overline{n}\right), \mathbf{W}\right]}{\overline{W}} = \frac{\mathrm{cov}\left(\mathbf{W}_{\mathbf{A}}, \mathbf{W}\right)}{\overline{W}} \tag{6}$$

This model is useful for describing the causal effects of and interactions between heritable variation in specific phenotypes $\boldsymbol{\eta}_{\mathbf{A}}$ using selection gradients $\boldsymbol{\beta}_{\mathbf{N}}$ and $\boldsymbol{\beta}_{\mathbf{S}}$. However, it is challenging to accurately estimate such high-dimensional, multivariate models in empirical research, due to bias caused by missing traits and poorly specified functional interactions (*91*).

Fortunately, an equivalent but lower dimensional model can be specified using a variance-partitioning approach. Rather than focusing on estimating all the specific genetic, social, and ecological interactions that shape every phenotype affecting an individual's fitness, a (co)variance-based model can be estimated to capture the total DGE W_D and IGE W'_I on individual fitness. These variance components summarize the net effects of directional selection acting on all heritable variation across phenotypes, partitioned from environmental effects ϵ on fitness

$$\begin{aligned} W_{jk} &= W_0 + \overline{W}\left(\boldsymbol{\beta}_{\mathbf{N}}^{\mathbf{T}}\boldsymbol{\eta}_{\mathbf{Aj}} + \boldsymbol{\beta}_{\mathbf{S}}^{\mathbf{T}}\overline{\boldsymbol{\eta}_{\mathbf{Ak}}}' n_k\right) + \epsilon_{jk} \\ &= W_0 + W_{D_j} + \sum_i^{n_k} W'_{I_i} + \epsilon_{jk} \\ &= W_0 + W_{D_j} + W'_{I_k|n} + \epsilon_{jk} \end{aligned} \tag{7}$$

where $W'_{I_k|n}$ is the total fitness effect of n social partners in neighborhood k of individual j. This shows, as noted in Fig. 1A, that the magnitude of social selection acting on heritable variation in all fitness-relevant phenotypes is proportional to the total IGE from social partners on focal fitness

$$W'_{I_k|n} \propto \boldsymbol{\beta}_{\mathbf{S}}^{\mathbf{T}}\boldsymbol{\eta}'_{\mathbf{Ak}} \tag{8}$$

These results also show that the contribution of $\boldsymbol{\beta}_{\mathbf{S}}^{\mathbf{T}}\boldsymbol{\eta}_{\mathbf{Aj}}$ to the total additive genetic value of fitness W_{Aj} will necessarily be 0 if there is no social selection $\boldsymbol{\beta}_{\mathbf{S}} = \mathbf{0}$ acting across phenotypes. Therefore, $\mathrm{var}\left(\mathbf{W}_{\mathbf{I}}\right) \neq 0$ in turn implies that there is a nonzero, net force of social selection acting across fitness-relevant phenotypes.

We can also see from applying Eq. 5 to Eqs. 7 and 8 that the absence of social plasticity in fitness-relevant phenotypes $\boldsymbol{\Psi} = \mathbf{0}$ will tend to reduce the magnitude of IGEs on fitness. In the strict sense, this means that observing $\mathrm{var}\left(\mathbf{W}_{\mathbf{I}}\right) \neq 0$ does not necessarily imply the existence of social plasticity in fitness relevant phenotypes, as the fitness IGE could be entirely driven by social selection in the absence of social plasticity. However, given the vast amount of evidence for socioecological plasticity in human reproduction and fitness-relevant behavior [e.g., (*12*, *13*, *21*, *51*, *52*, *60*, *62*, *63*, *92*–*94*)], we assume as an empirical fact that many elements of $\boldsymbol{\Psi}$ will always be nonzero in any human population and will thus be contributing to the total additive genetic values of fitness-relevant traits determining the fertility of individuals $\boldsymbol{\eta}_{\mathbf{A}}$ and their social partners $\boldsymbol{\eta}'_{\mathbf{A}}$. We, therefore, interpret $\mathrm{var}\left(\mathbf{W}_{\mathbf{I}}\right) \neq 0$ as indicating that a net force of social selection is occurring across heritable variation in fitness-relevant phenotypes and that, as a consequence, social plasticity in these phenotypes is also affecting the additive genetic variance of fitness via IGEs.

Using Eq. 7, the marginal IGE of an individual on a single social partner is defined by

$$\mathrm{W}_{Ij} = \frac{W_{I_j|\overline{n}}}{\overline{n}} \tag{9}$$

As explained above in Eqs. 1A to 1E, these individual-level DGEs and IGEs can be efficiently estimated using a social animal model (*58*) where the fitness component itself is the trait being selected on (*41*). Using latent variable W_α to capture correlated genetic effects on focal and partner fitness

$$W_{jk} = W_0 + W_{D_j} + W'_{I_k|n} + \epsilon_{jk} = W_0 + \beta_{\mathrm{NW}} W_{\alpha_j} + \beta_{\mathrm{SW}}\ \overline{W'_{\alpha k}} n_k + \epsilon_{jk} \tag{10}$$

we fix $\beta_{\mathrm{NW}} = 1$ to identify the latent variable, such that $1 * W_{\alpha_j} = W_{Dj}$ and

$$\begin{aligned} W_{jk} &= W_0 + \overline{W}\left(\boldsymbol{\beta}_{\mathbf{N}}^{\mathbf{T}}\boldsymbol{\eta}_{\mathbf{Aj}} + \boldsymbol{\beta}_{\mathbf{S}}^{\mathbf{T}}\overline{\boldsymbol{\eta}_{\mathbf{Ak}}}' n_k\right) + \epsilon_{jk} \\ &= W_0 + W_{D_j} + W'_{I_k|n} + \epsilon_{jk} \\ &= W_0 + W_{D_j} + \beta_{\mathrm{SW}}\ \overline{W'_{Dk}} n_k + \epsilon_{jk} \end{aligned} \tag{11}$$

where $\beta_{\mathrm{SW}}\ \overline{W'_{Dk}} n_k$ quantifies the fitness IGE of social partners, as shown in Fig. 3A. Genetic (co)variances of total IGEs on fitness across the population can then be calculated as

$$\begin{aligned} \mathrm{var}\left(\overline{W}\boldsymbol{\beta}_{\mathbf{S}}^{\mathbf{T}}\boldsymbol{\eta}_{\mathbf{A}}\overline{n}\right) &= \mathrm{var}\left(\mathbf{W}_{\mathbf{I}|\overline{n}}\right) = \mathrm{var}\left(\mathbf{W}_{\mathbf{D}}\right)\beta_{\mathrm{SW}}^2\overline{n}^2 \\ \mathrm{cov}\left(\overline{W}\boldsymbol{\beta}_{\mathbf{N}}^{\mathbf{T}}\boldsymbol{\eta}_{\mathbf{A}}, \overline{W}\boldsymbol{\beta}_{\mathbf{S}}^{\mathbf{T}}\boldsymbol{\eta}_{\mathbf{A}}\right) &= \mathrm{cov}\left(\mathbf{W}_{\mathbf{D}}, \mathbf{W}_{\mathbf{I}}\right) = \mathrm{var}\left(\mathbf{W}_{\mathbf{D}}\right)\beta_{\mathrm{SW}} \end{aligned} \tag{12}$$

As shown in Fig. 1 (A and B), this indicates that social selection estimated by the regression of focal fitness on partner fitness β_{SW} is proportional to the net effect of social selection to either increase cooperation $\mathrm{cov}(\mathbf{W_D}, \mathbf{W_I}) > 0$ or increase conflict $\mathrm{cov}(\mathbf{W_D}, \mathbf{W_I}) < 0$ in fitness across fitness-relevant phenotypes.

$$\beta_{SW} \propto \mathrm{cov}(\mathbf{W_D}, \mathbf{W_I}) \propto \mathrm{cov}(\boldsymbol{\beta}_\mathbf{N}^\mathbf{T}\boldsymbol{\eta}_\mathbf{A}, \boldsymbol{\beta}_\mathbf{S}^\mathbf{T}\boldsymbol{\eta}_\mathbf{A}) \tag{13}$$

The total additive genetic value for j in the variance partitioning model (Eq. 7) is

$$W_{Aj} = \overline{W}(\boldsymbol{\beta}_\mathbf{N}^\mathbf{T}\boldsymbol{\eta}_\mathbf{Aj} + \boldsymbol{\beta}_\mathbf{S}^\mathbf{T}\,\boldsymbol{\eta}_\mathbf{Aj}\overline{n}) = W_{Dj} + W_{Ij}\overline{n} \tag{14}$$

which again is the heritable effect of the phenotypes of individual j on mean population fitness, holding average allele effects and environmental distributions constant. Using Eq. 6, the adaptive response to heritable variation in fitness can then be estimated by

$$\Delta\overline{W} = \frac{\mathrm{cov}[\overline{W}(\boldsymbol{\beta}_\mathbf{N}^\mathbf{T}\boldsymbol{\eta}_\mathbf{A} + \boldsymbol{\beta}_\mathbf{S}^\mathbf{T}\boldsymbol{\eta}_\mathbf{A}\overline{n}), \mathbf{W}]}{\overline{W}} = \frac{\mathrm{cov}\left(\mathbf{W_D} + \mathbf{W_I}\overline{n}, \mathbf{W_D} + \mathbf{W'_{I|\overline{n}}}\right)}{\overline{W}} \tag{15}$$

From this perspective, it is easier to see that the adaptive response to heritable fitness variation (i.e., the net effects of selection across all heritable phenotypes) will be contingent on the genetic integration of fitness DGEs and IGEs within individuals $\mathrm{cov}(\mathbf{W_D}, \mathbf{W_I})$, as well as the expected relatedness $\bar{r}$ between individuals and the indirect effects of their social partners $\mathbf{W'_{I|\overline{n}}}$. For symmetric social interactions

$$\begin{aligned} \mathrm{cov}\left(\mathbf{W_D}, \mathbf{W'_{I|\overline{n}}}\right) &= \bar{r}\,\mathrm{cov}(\mathbf{W_D}, \mathbf{W_I})\overline{n} \\ \mathrm{cov}\left(\mathbf{W_I}, \mathbf{W'_{I|\overline{n}}}\right) &= \bar{r}\,\mathrm{var}(\mathbf{W_I})\overline{n}^2 = \bar{r}\,\mathrm{var}(\mathbf{W_{I|\overline{n}}}) \end{aligned} \tag{16}$$

Following prior work by Bijma (*40*), the change in population fitness can then be predicted from the (co)variation of estimated fitness DGEs and IGEs such that

$$\Delta\overline{W} = \frac{\mathrm{cov}(\mathbf{W_A}, \mathbf{W})}{\overline{W}} = \frac{\mathrm{var}(\mathbf{W_D}) + \overline{n}\,\mathrm{cov}(\mathbf{W_D}, \mathbf{W_I}) + \bar{r}\left[\mathrm{var}(\mathbf{W_{I|\overline{n}}}) + \overline{n}\,\mathrm{cov}(\mathbf{W_D}, \mathbf{W_I})\right]}{\overline{W}} \tag{17}$$

where change due to $\overline{n}\,\mathrm{cov}(\mathbf{W_D}, \mathbf{W_I})$ is a consequence of correlated evolution in mean fitness caused by change in the mean DGE $\overline{W}_D$, and $\bar{r}\left[\mathrm{var}(\mathbf{W_{I|\overline{n}}}) + \overline{n}\,\mathrm{cov}(\mathbf{W_D}, \mathbf{W_I})\right]$ are inclusive fitness effects caused by relatedness among social partners. The evolvability of fitness—i.e., the potential for an adaptive genetic response to selection (*34*)—can thus be estimated by

$$e_{W|\bar{r}} = \frac{\mathrm{var}(\mathbf{W_D}) + \overline{n}\,\mathrm{cov}(\mathbf{W_D}, \mathbf{W_I}) + \bar{r}\left[\mathrm{var}(\mathbf{W_{I|\overline{n}}}) + \overline{n}\,\mathrm{cov}(\mathbf{W_D}, \mathbf{W_I})\right]}{\overline{W}^2} \tag{18}$$

contingent on the average relatedness $\bar{r}$ and number of social partners $\overline{n}$. Scaling the evolvability by the squared mean fitness $\overline{W}^2$ allows for straightforward interpretation of $100{*}e_{W|\bar{r}}$ as the expected % change in the heritable component of fitness in one generation (*95*). Note that this expression can also be generalized to other heritable sources of direct W_D and indirect W_I effects on fitness, such as mechanisms of cultural or ecological inheritance, by substituting in an appropriate scaling matrix for $\mathbf{A}$ in Eq. 1B along with a phenotypic assortment coefficient β_α for the genetic relatedness coefficient r in Eqs. 16 to 18, capturing any repeatable causes of phenotypic similarity among partners in the evolving trait value (*54*).

Some of this genetic response in average fitness is due to indirect effects on the fitness of unrelated social partners, which from an inclusive fitness and gene's eye perspective can be considered a by-product of environmental change induced by selection rather than a direct component of adaptation and fitness maximization (*41*). Following (*40*), we can, therefore, also define an inclusive fitness (IF) evolvability quotient $e_{W_{IF}|\bar{r}}$ that only accounts for average genetic effects on the fitness of related group members

$$e_{W_{IF}|\bar{r}} = \frac{\mathrm{var}(\mathbf{W_D}) + \bar{r}\left[\mathrm{var}(\mathbf{W_{I|\overline{n}}}) + 2\overline{n}\,\mathrm{cov}(\mathbf{W_D}, \mathbf{W_I})\right]}{\overline{W}^2} \tag{19}$$

This shows that quantitative genetic effects of magnitude

$$e_{W|\bar{r}} - e_{W_{IF}|\bar{r}} = \frac{\overline{n}\left[\mathrm{cov}(\mathbf{W_D}, \mathbf{W_I}) - \bar{r}\,\mathrm{cov}(\mathbf{W_D}, \mathbf{W_I})\right]}{\overline{W}^2} \tag{20}$$

will shape intergenerational change in mean fitness as a genetically correlated response to directional selection on average fitness DGEs and IGEs among related social partners. To more directly test whether social interactions are accelerating or inhibiting the rate of adaptation in fertility, a null hypothesis nonsocial evolvability quotient

$$e_{W0} = \frac{\mathrm{var}(\mathbf{W_D})}{\overline{W}^2} \tag{21}$$

can be used to predict the rate of adaptation in the absence (0) of IGEs caused by social plasticity and social selection among women. The increase in the inclusive fitness of the population via plastic and interdependent social interactions $e_{W_{IF}|\bar{r}} - e_{W0}$ will thus be proportional to $\bar{r}\left[\mathrm{var}(\mathbf{W_{I|\overline{n}}}) + 2\overline{n}\,\mathrm{cov}(\mathbf{W_D}, \mathbf{W_I})\right]$, with indirect selection effects $\overline{n}\left[\mathrm{cov}(\mathbf{W_D}, \mathbf{W_I}) - \bar{r}\,\mathrm{cov}(\mathbf{W_D}, \mathbf{W_I})\right]$ potentially further accelerating or reducing the expected change in the instantaneous rate of intrinsic population growth (i.e., the genetic adaptation of mean fitness).

Supplementary Materials

This PDF file includes:

Supplementary Text
Figs. S1 and S2
References

REFERENCES AND NOTES

1. K. R. Hill, R. S. Walker, M. Bozicević, J. Eder, T. Headland, B. Hewlett, A. M. Hurtado, F. Marlowe, P. Wiessner, B. Wood, Co-residence patterns in hunter-gatherer societies show unique human social structure. *Science* **331**, 1286–1289 (2011).
2. C. T. Ross, P. L. Hooper, J. E. Smith, A. V. Jaeggi, E. A. Smith, S. Gavrilets, F. T. Zohora, J. Ziker, D. Xygalatas, E. E. Wroblewski, B. Wood, B. Winterhalder, K. P. Willführ, A. K. Willard, K. Walker, C. von Rueden, E. Voland, C. Valeggia, B. Vaitla, S. Urlacher, M. Towner, C.-Y. Sum, L. S. Sugiyama, K. B. Strier, K. Starkweather, D. Major-Smith, M. Shenk, R. Sear, E. Seabright, R. Schacht, B. Scelza, S. Scaggs, J. Salerno, C. Revilla-Minaya, D. Redhead, A. Pusey, B. G. Purzycki, E. A. Power, A. Pisor, J. Pettay, S. Perry, A. E. Page, L. Pacheco-Cobos, K. Oths, S.-Y. Oh, D. Nolin, D. Nettle, C. Moya, A. B. Migliano, K. J. Mertens, R. A. McNamara, R. McElreath, S. Mattison, E. Massengill, F. Marlowe,

F. Madimenos, S. Macfarlan, V. Lummaa, R. Lizarralde, R. Liu, M. A. Liebert, S. Lew-Levy, P. Leslie, J. Lanning, K. Kramer, J. Koster, H. S. Kaplan, B. Jamsranjav, A. M. Hurtado, K. Hill, B. Hewlett, S. Helle, T. Headland, J. Headland, M. Gurven, G. Grimalda, R. Greaves, C. D. Golden, I. Godoy, M. Gibson, C. E. Mouden, M. Dyble, P. Draper, S. Downey, A. L. DeMarco, H. E. Davis, S. Crabtree, C. Cortez, H. Colleran, E. Cohen, G. Clark, J. Clark, M. A. Caudell, C. E. Carminito, J. Bunce, A. Boyette, S. Bowles, T. Blumenfield, B. Beheim, S. Beckerman, Q. Atkinson, C. Apicella, N. Alam, M. B. Mulder, Reproductive inequality in humans and other mammals. *Proc. Natl. Acad. Sci. U.S.A.* **120**, e2220124120 (2023).

3. J. Prado-Martinez, P. H. Sudmant, J. M. Kidd, H. Li, J. L. Kelley, B. Lorente-Galdos, K. R. Veeramah, A. E. Woerner, T. D. O'Connor, G. Santpere, A. Cagan, C. Theunert, F. Casals, H. Laayouni, K. Munch, A. Hobolth, A. E. Halager, M. Malig, J. Hernandez-Rodriguez, I. Hernando-Herraez, K. Prüfer, M. Pybus, L. Johnstone, M. Lachmann, C. Alkan, D. Twigg, N. Petit, C. Baker, F. Hormozdiari, M. Fernandez-Callejo, M. Dabad, M. L. Wilson, L. Stevison, C. Camprubí, T. Carvalho, A. Ruiz-Herrera, L. Vives, M. Mele, T. Abello, I. Kondova, R. E. Bontrop, A. Pusey, F. Lankester, J. A. Kiyang, R. A. Bergl, E. Lonsdorf, S. Myers, M. Ventura, P. Gagneux, D. Comas, H. Siegismund, J. Blanc, L. Agueda-Calpena, M. Gut, L. Fulton, S. A. Tishkoff, J. C. Mullikin, R. K. Wilson, I. G. Gut, M. K. Gonder, O. A. Ryder, B. H. Hahn, A. Navarro, J. M. Akey, J. Bertranpetit, D. Reich, T. Mailund, M. H. Schierup, C. Hvilsom, A. M. Andrés, J. D. Wall, C. D. Bustamante, M. F. Hammer, E. E. Eichler, T. Marques-Bonet, Great ape genetic diversity and population history. *Nature* **499**, 471–475 (2013).
4. S. A. Frank, *Foundations of Social Evolution* (Princeton Univ. Press, 1998).
5. R. Boyd, P. J. Richerson, Large-scale cooperation in small-scale foraging societies. *Evol. Anthropol.* **31**, 175–198 (2022).
6. S. C. Antón, R. Potts, L. C. Aiello, Human evolution., Evolution of early Homo: An integrated biological perspective. *Science* **345**, 1236828 (2014).
7. K. Hill, M. Barton, A. M. Hurtado, The emergence of human uniqueness: Characters underlying behavioral modernity. *Evol. Anthropol.* **18**, 187–200 (2009).
8. K. L. Kramer, How there got to be so many of us: The evolutionary story of population growth and a life history of cooperation. *J. Anthropol. Res.* **75**, 472–497 (2019).
9. M. D. Gurven, R. J. Davison, Periodic catastrophes over human evolutionary history are necessary to explain the forager population paradox. *Proc. Natl. Acad. Sci. U.S.A.* **116**, 12758–12766 (2019).
10. R. S. Walker, M. Gurven, O. Burger, M. J. Hamilton, The trade-off between number and size of offspring in humans and other primates. *Proc. Biol. Sci.* **275**, 827–833 (2008).
11. I. F. Miller, S. E. Churchill, C. L. Nunn, Speeding in the slow lane: Phylogenetic comparative analyses reveal that not all human life history traits are exceptional. *J. Hum. Evol.* **130**, 36–44 (2019).
12. J. S. Martin, E. J. Ringen, P. Duda, A. V. Jaeggi, Harsh environments promote alloparental care across human societies. *Proc. Biol. Sci.* **287**, 20200758 (2020).
13. M. Gurven, To give and to give not: The behavioral ecology of human food transfers. *Behav. Brain Sci.* **27**, 543–559 (2004).
14. C. R. Ember, I. Skoggard, E. J. Ringen, M. Farrer, Our better nature: Does resource stress predict beyond-household sharing? *Evol. Hum. Behav.* **39**, 380–391 (2018).
15. E. A. Cashdan, Egalitarianism among hunters and gatherers. *Am. Anthropol.* **82**, 116–120 (1980).
16. M. Borgerhoff Mulder, S. Bowles, T. Hertz, A. Bell, J. Beise, G. Clark, I. Fazzio, M. Gurven, K. Hill, P. L. Hooper, W. Irons, H. Kaplan, D. Leonetti, B. Low, F. Marlowe, R. McElreath, S. Naidu, D. Nolin, P. Piraino, R. Quinlan, E. Schniter, R. Sear, M. Shenk, E. A. Smith, C. von Rueden, P. Wiessner, Intergenerational wealth transmission and the dynamics of inequality in small-scale societies. *Science* **326**, 682–688 (2009).
17. A. Aktipis, L. Cronk, J. Alcock, J. D. Ayers, C. Baciu, D. Balliet, A. M. Boddy, O. S. Curry, J. A. Krems, A. Muñoz, D. Sullivan, D. Sznycer, G. S. Wilkinson, P. Winfrey, Understanding cooperation through fitness interdependence. *Nat. Hum. Behav.* **2**, 429–431 (2018).
18. H. S. Kaplan, P. L. Hooper, M. Gurven, The evolutionary and ecological roots of human social organization. *Philos. Trans. R Soc. Lond. B Biol. Sci.* **364**, 3289–3299 (2009).
19. T. Clutton-Brock, Breeding together: Kin selection and mutualism in cooperative vertebrates. *Science* **296**, 69–72 (2002).
20. S. A. West, G. A. Cooper, M. B. Ghoul, A. S. Griffin, Ten recent insights for our understanding of cooperation. *Nat. Ecol. Evol.* **5**, 419–430 (2021).
21. P. J. Richerson, R. Boyd, *Not by Genes Alone: How Culture Transformed Human Evolution* (Chicago: University of Chicago Press, 2004).
22. K. Sterelny, Humans as model organisms. *Proc. Biol. Sci.* **284**, 20172115 (2017).
23. M. L. Wilson, C. M. Miller, K. N. Crouse, Humans as a model species for sexual selection research. *Proc. Biol. Sci.* **284**, 20171320 (2017).
24. H. C. Barrett, Deciding what to observe: Thoughts for a post-WEIRD generation. *Evol. Hum. Behav.* **41**, 445–453 (2020).
25. A. Hendry, *Eco-evolutionary dynamics* (reprint edition) (Princeton Univ. Press, 2020).
26. R. Ferriere, S. Legendre, Eco-evolutionary feedbacks, adaptive dynamics and evolutionary rescue theory. *Philos. Trans. R Soc. Lond. B Biol. Sci.* **368**, 20120081 (2013).
27. C. Wood, R. N. L. Fitt, L. T. Lancaster, Evolving social dynamics prime thermal tolerance during a poleward range shift. *Biol. J. Linn. Soc.* **126**, 574–586 (2019).
28. G. J. B. Henriques, M. M. Osmond, Cooperation can promote rescue or lead to evolutionary suicide during environmental change. *Evolution* **74**, 1255–1273 (2020).
29. S. P. Carroll, A. P. Hendry, D. N. Reznick, C. W. Fox, Evolution on ecological time-scales. *Funct. Ecol.* **21**, 387–393 (2007).
30. T. Bonnet, M. B. Morrissey, P. de Villemereuil, S. C. Alberts, P. Arcese, L. D. Bailey, S. Boutin, P. Brekke, L. J. N. Brent, G. Camenisch, A. Charmantier, T. H. Clutton-Brock, A. Cockburn, D. W. Coltman, A. Courtiol, E. Davidian, S. R. Evans, J. G. Ewen, M. Festa-Bianchet, C. de Franceschi, L. Gustafsson, O. P. Höner, T. M. Houslay, L. F. Keller, M. Manser, A. G. McAdam, E. McLean, P. Nietlisbach, H. L. Osmond, J. M. Pemberton, E. Postma, J. M. Reid, A. Rutschmann, A. W. Santure, B. C. Sheldon, J. Slate, C. Teplitsky, M. E. Visser, B. Wachter, L. E. B. Kruuk, Genetic variance in fitness indicates rapid contemporary adaptive evolution in wild animals. *Science* **376**, 1012–1016 (2022).
31. R. A. Fisher, *The Genetical Theory of Natural Selection* (Oxford Univ. Press, 1930).
32. A. J. Moore, E. D. Brodie III, J. B. Wolf, Interacting phenotypes and the evolutionary process: I. direct and indirect genetic effects of social interactions. *Evolution* **51**, 1352–1362 (1997).
33. P. Bijma, M. J. Wade, The joint effects of kin, multilevel selection and indirect genetic effects on response to genetic selection. *J. Evol. Biol.* **21**, 1175–1188 (2008).
34. T. F. Hansen, C. Pélabon, Evolvability: A quantitative-genetics perspective. *Annu. Rev. Ecol. Evol. Syst.* **52**, 153–175 (2021).
35. M. J. Wade, Group selections among laboratory populations of Tribolium. *Proc. Natl. Acad. Sci. U.S.A.* **73**, 4604–4607 (1976).
36. M. J. Wade, P. Bijma, E. D. Ellen, W. Muir, Group selection and social evolution in domesticated animals. *Evol. Appl.* **3**, 453–465 (2010).
37. E. M. McLean, J. A. Moorad, J. Tung, E. A. Archie, S. C. Alberts, Genetic variance and indirect genetic effects for affiliative social behavior in a wild primate. *Evolution* **77**, 1607–1621 (2023).
38. J. W. McGlothlin, A. J. Moore, J. B. Wolf, E. D. Brodie III, Interacting phenotypes and the evolutionary process. III. Social evolution. *Evolution* **64**, 2558–2574 (2010).
39. D. N. Fisher, A. G. McAdam, Indirect genetic effects clarify how traits can evolve even when fitness does not. *Evol. Lett.* **3**, 4–14 (2019).
40. P. Bijma, Fisher's fundamental theorem of inclusive fitness and the change in fitness due to natural selection when conspecifics interact. *J. Evol. Biol.* **23**, 194–206 (2010).
41. J. W. McGlothlin, D. N. Fisher, Social selection and the evolution of maladaptation. *J. Hered.* **113**, 61–68 (2022).
42. S. F. Chenoweth, H. D. Rundle, M. W. Blows, Experimental evidence for the evolution of indirect genetic effects: Changes in the interaction effect coefficient, psi (Psi), due to sexual selection. *Evolution* **64**, 1849–1856 (2010).
43. S. Andersson, Indirect genetic effects from competition in the clonal herb Sedum album (Crassulaceae). *PLOS ONE* **9**, e106104 (2014).
44. M. J. Carter, A. J. Wilson, A. J. Moore, N. J. Royle, The role of indirect genetic effects in the evolution of interacting reproductive behaviors in the burying beetle, *Nicrophorus vespilloides*. *Ecol. Evol.* **9**, 998–1009 (2019).
45. F. Santostefano, M. Moiron, A. Sánchez-Tójar, D. N. Fisher, Indirect genetic effects increase the heritable variation available to selection and are largest for behaviors: A meta-analysis. *Evol. Lett.* **9**, 89–104 (2025).
46. A. J. Wilson, M. B. Morrissey, M. J. Adams, C. A. Walling, F. E. Guinness, J. M. Pemberton, T. H. Clutton-Brock, L. E. B. Kruuk, Indirect genetics effects and evolutionary constraint: An analysis of social dominance in red deer, Cervus elaphus. *J. Evol. Biol.* **24**, 772–783 (2011).
47. S. R. Evans, D. Waldvogel, N. Vasiljevic, E. Postma, Heritable spouse effects increase evolutionary potential of human reproductive timing. *Proc. Biol. Sci.* **285**, 20172763 (2018).
48. C. Xia, O. Canela-Xandri, K. Rawlik, A. Tenesa, Evidence of horizontal indirect genetic effects in humans. *Nat. Hum. Behav.* **5**, 399–406 (2021).
49. F. Santostefano, H. Allegue, D. Garant, P. Bergeron, D. Réale, Indirect genetic and environmental effects on behaviors, morphology, and life-history traits in a wild Eastern chipmunk population. *Evolution* **75**, 1492–1512 (2021).
50. J. A. Moorad, C. A. Walling, Measuring selection for genes that promote long life in a historical human population. *Nat. Ecol. Evol.* **1**, 1773–1781 (2017).
51. C. W. Kuzawa, J. M. Bragg, Plasticity in human life history Strategy. *Curr. Anthropol.* **53**, S369–S382 (2012).
52. R. Sear, D. W. Lawson, H. Kaplan, M. K. Shenk, Understanding variation in human fertility: What can we learn from evolutionary demography? *Philos. Trans. R Soc. Lond. B Biol. Sci.* **371**, 20150144 (2016).
53. F. C. Tropf, S. H. Lee, R. M. Verweij, G. Stulp, P. J. van der Most, R. de Vlaming, A. Bakshi, D. A. Briley, C. Rahal, R. Hellpap, A. N. Iliadou, T. Esko, A. Metspalu, S. E. Medland, N. G. Martin, N. Barban, H. Snieder, M. R. Robinson, M. C. Mills, Hidden heritability due to heterogeneity across seven populations. *Nat. Hum. Behav.* **1**, 757–765 (2017).
54. J. S. Martin, A. V. Jaeggi, S. E. Koski, The social evolution of individual differences: Future directions for a comparative science of personality in social behavior. *Neurosci. Biobehav. Rev.* **144**, 104980 (2023).

55. J. S. Martin, D. Westneat, A. J. Wilson, N. J. Dingemanse, Y. G. Araya-Ajoy, Frequency-dependence favors social plasticity and facilitates socio-eco-evolutionary feedback in fluctuating environments. EcoEvoRxiv X2KW5R [Preprint] (2024). https://doi.org/10.32942/X2KW5R.
56. N. W. Bailey, C. Desjonquères, A. Drago, J. G. Rayner, S. L. Sturiale, X. Zhang, A neglected conceptual problem regarding phenotypic plasticity's role in adaptive evolution: The importance of genetic covariance and social drive. *Evol. Lett.* **5**, 444–457 (2021).
57. E. Crispo, The Baldwin effect and genetic assimilation: Revisiting two mechanisms of evolutionary change mediated by phenotypic plasticity. *Evolution* **61**, 2469–2479 (2007).
58. J. S. Martin, A. V. Jaeggi, Social animal models for quantifying plasticity, assortment, and selection on interacting phenotypes. *J. Evol. Biol.* **35**, 520–538 (2022).
59. M. Gurven, J. Stieglitz, B. Trumble, A. D. Blackwell, B. Beheim, H. Davis, P. Hooper, H. Kaplan, The Tsimane Health and Life History Project: Integrating anthropology and biomedicine. *Evol. Anthropol.* **26**, 54–73 (2017).
60. A. V. Jaeggi, P. L. Hooper, B. A. Beheim, H. Kaplan, M. Gurven, Reciprocal exchange patterned by market forces helps explain cooperation in a small-scale society. *Curr. Biol.* **26**, 2180–2187 (2016).
61. A. P. Hendry, D. J. Schoen, M. E. Wolak, J. M. Reid, The Contemporary evolution of fitness. *Annu. Rev. Ecol. Evol. Syst.* **49**, 457–476 (2018).
62. E. A. Smith, B. Winterhalder, *Evolutionary Ecology and Human Behavior* (Routledge, 1992).
63. A. E. Page, M. G. Thomas, D. Smith, M. Dyble, S. Viguier, N. Chaudhary, G. D. Salali, J. Thompson, R. Mace, A. B. Migliano, Testing adaptive hypotheses of alloparenting in Agta foragers. *Nat. Hum. Behav.* **3**, 1154–1163 (2019).
64. S. T. Powers, C. P. van Schaik, L. Lehmann, Cooperation in large-scale human societies-What, if anything, makes it unique, and how did it evolve? *Evol. Anthropol.* **30**, 280–293 (2021).
65. L. E. B. Kruuk, J. D. Hadfield, How to separate genetic and environmental causes of similarity between relatives. *J. Evol. Biol.* **20**, 1890–1903 (2007).
66. M. Gurven, J. Winking, H. Kaplan, C. von Rueden, L. McAllister, A bioeconomic approach to marriage and the sexual division of labor. *Hum. Nat.* **20**, 151–183 (2009).
67. P. L. Hooper, M. Gurven, J. Winking, H. S. Kaplan, Inclusive fitness and differential productivity across the life course determine intergenerational transfers in a small-scale human society. *Proc. Biol. Sci.* **282**, 20142808 (2015).
68. M. H. D. Larmuseau, K. Matthijs, T. Wenseleers, Cuckolded fathers rare in human populations. *Trends Ecol. Evol.* **31**, 327–329 (2016).
69. A. Charmantier, D. Réale, How do misassigned paternities affect the estimation of heritability in the wild? *Mol. Ecol.* **14**, 2839–2850 (2005).
70. J. D. Hadfield, MCMC methods for multi-response generalized linear mixed models: The MCMCglmm R package. *J. Stat. Softw. 33*, 1–22 (2010).
71. M. Gurven, A. Zanolini, E. Schniter, Culture sometimes matters: Intra-cultural variation in pro-social behavior among Tsimane Amerindians. *J. Econ. Behav. Organ.* **67**, 587–607 (2008).
72. E. Seabright, S. Alami, T. S. Kraft, H. Davis, A. E. Caldwell, P. Hooper, L. McAllister, S. Mulville, A. Veila, C. von Rueden, B. Trumble, J. Stieglitz, M. Gurven, H. Kaplan, Repercussions of patrilocal residence on mothers' social support networks among Tsimane forager-farmers. *Philos. Trans. R. Soc. Lond. B Biol. Sci.* **378**, 20210442 (2023).
73. C.-D. Mayer, J. Lorent, G. W. Horgan, Exploratory analysis of multiple omics datasets using the adjusted RV coefficient. *Stat. Appl. Genet. Mol. Biol.* **10**, 10.2202/1544-6115.1540 (2011).
74. P. Bijma, The quantitative genetics of indirect genetic effects: A selective review of modelling issues. *Heredity* **112**, 61–69 (2014).
75. B. Carpenter, A. Gelman, M. D. Hoffman, D. Lee, B. Goodrich, M. Betancourt, M. A. Brubaker, J. Guo, P. Li, A. Riddell, Stan: A probabilistic programming language. *J. Stat. Softw.* **76**, 1 (2017).
76. R Core Team. *R: A language and environment for statistical computing* (R Foundation for Statistical Computing, 2021); https://R-project.org/.
77. J. Gabry. R. Češnovar, A. Johnson. cmdstanr: R Interface to 'CmdStan'. (2023); https://mc-stan.org/cmdstanr/.
78. H. Schielzeth, Simple means to improve the interpretability of regression coefficients. *Methods Ecol. Evol.* **1**, 103–113 (2010).
79. R. McElreath. *Statistical Rethinking: A Bayesian Course with Examples in R and Stan* (CRC Press, ed. 2, 2020).
80. Stan Development Team. *Stan Modeling Language Users Guide and Reference Manual*, Version 2.34. (2024); https://mc-stan.org.
81. N. P. Lemoine, Moving beyond noninformative priors: Why and how to choose weakly informative priors in Bayesian analyses. *Oikos* **128**, 912–928 (2019).
82. B. B. McShane, D. Gal, A. Gelman, C. Robert, J. L. Tackett, Abandon statistical significance. *Am. Stat.* **73**, 235–245 (2019).
83. M. Turelli, N. H. Barton, Genetic and statistical analyses of strong selection on polygenic traits: What, me normal? *Genetics* **138**, 913–941 (1994).
84. Y. G. Araya-Ajoy, D. F. Westneat, J. Wright, Pathways to social evolution and their evolutionary feedbacks. *Evolution* **74**, 1894–1907 (2020).
85. J. D. Hadfield, A. J. Wilson, D. Garant, B. C. Sheldon, L. E. B. Kruuk, The misuse of BLUP in ecology and evolution. *Am. Nat.* **175**, 116–125 (2010).
86. J. R. Stinchcombe, A. K. Simonsen, M. W. Blows, Estimating uncertainty in multivariate responses to selection. *Evolution* **68**, 1188–1196 (2014).
87. T. F. Hereford, D. Hansen, D. Houle, Comparing strengths of directional selection: How strong is strong? *Evolution* **58**, 2133–2143 (2004).
88. H. A. Orr, Fitness and its role in evolutionary genetics. *Nat. Rev. Genet.* **10**, 531–539 (2009).
89. A. Robertson, A mathematical model of the culling process in dairy cattle. *Anim. Sci.* **8**, 95–108 (1966).
90. G. R. Price, Extension of covariance selection mathematics. *Ann. Hum. Genet.* **35**, 485–490 (1972).
91. M. B. Morrissey, L. E. B. Kruuk, A. J. Wilson, The danger of applying the breeder's equation in observational studies of natural populations. *J. Evol. Biol.* **23**, 2277–2288 (2010).
92. R. Sear, R. Mace, Who keeps children alive? A review of the effects of kin on child survival. *Evol. Hum. Behav.* **29**, 1–18 (2008).
93. J. Henrich, Culture and social behavior. *Curr. Opin. Behav. Sci.* **3**, 84–89 (2015).
94. J. Henrich, M. Muthukrishna, The origins and psychology of human cooperation. *Annu. Rev. Psychol.* **72**, 207–240 (2021).
95. T. F. Hansen, C. Pélabon, D. Houle, Heritability is not evolvability. *Evol. Biol.* **38**, 258–277 (2011).
96. R. G. Shaw, F. H. Shaw, Quantitative genetic study of the adaptive process. *Heredity* **112**, 13–20 (2014).
97. S. C. Stearns, *The Evolution of Life Histories* (OUP Oxford, 1992).
98. J. E. Brommer, J. Merilä, H. Kokko, Reproductive timing and individual fitness. *Ecol. Lett.* **5**, 802–810 (2002).
99. J. B. McGraw, H. Caswell, Estimation of individual fitness from life-history data. *Am. Nat.* **147**, 47–64 (1996).
100. J. A. Moorad, Individual fitness and phenotypic selection in age-structured populations with constant growth rates. *Ecology* **95**, 1087–1095 (2014).
101. J. A. Moorad, Multi-level sexual selection: Individual and family-level selection for mating success in a historical human population. *Evolution* **67**, 1635–1648 (2013).
102. J. A. Moorad, A demographic transition altered the strength of selection for fitness and age-specific survival and fertility in a 19th century American population. *Evolution* **67**, 1622–1634 (2013).
103. G. R. Price, Fisher's "fundamental theorem" made clear. *Ann. Hum. Genet.* **36**, 129–140 (1972).
104. T. R. Haaland, J. Wright, I. I. Ratikainen, Individual reversible plasticity as a genotype-level bet-hedging strategy. *J. Evol. Biol.* **34**, 1022–1033 (2021).
105. A. Burt, The evolution of fitness. *Evolution* **49**, 1–8 (1995).
106. H. Kaplan, P. L. Hooper, J. Stieglitz, M. Gurven, The causal relationship between fertility and infant mortality. *Pop. Hum. Sci.*, 361–376 (2015).
107. E. A. Young, E. Chesterton, V. Lummaa, E. Postma, H. L. Dugdale, The long-lasting legacy of reproduction: Lifetime reproductive success shapes expected genetic contributions of humans after 10 generations. *Proc. Biol. Sci.* **290**, 20230287 (2023).
108. S. Helle, J. E. Brommer, J. E. Pettay, V. Lummaa, M. Enbuske, J. Jokela, Evolutionary demography of agricultural expansion in preindustrial northern Finland. *Proc. Biol. Sci.* **281**, 20141559 (2014).
109. N. Pilakouta, E. J. H. Hanlon, P. T. Smiseth, Biparental care is more than the sum of its parts: Experimental evidence for synergistic effects on offspring fitness. *Proc. Biol. Sci.* **285**, 20180875 (2018).
110. I. Alger, P. L. Hooper, D. Cox, J. Stieglitz, H. S. Kaplan, Paternal provisioning results from ecological change. *Proc. Natl. Acad. Sci. U.S.A.* **117**, 10746–10754 (2020).
111. D. W. Bird, R. B. Bird, B. F. Codding, D. W. Zeanah, Variability in the organization and size of hunter-gatherer groups: Foragers do not live in small-scale societies. *J. Hum. Evol.* **131**, 96–108 (2019).
112. J. D. Hadfield, Estimating evolutionary parameters when viability selection is operating. *Proc. Biol. Sci.* **275**, 723–734 (2008).

Acknowledgments: We thank the many Tsimane research assistants who aided in data collection and the Tsimane participants who made this study possible. **Funding:** This work was supported by the University of Zurich Candoc/Forschungskredit grant number FK-20-034 (J.S.M.), the National Institute on Aging within the National Institutes of Health (R01AG054442), the National Science Foundation (1748282), and the French National Research Agency under the Investments for the Future (Investissements d'Avenir) programme (ANR-17-EURE0010).
Author contributions: Conceptualization: J.S.M. Methodology: J.S.M., A.V.J., B.B., M.G., H.K., B.C.T., and P.H. Software: J.S.M. and B.B. Validation: J.S.M., B.B., and D.C. Formal analysis: J.S.M. and B.B. Investigation: M.G., H.K., J.S., B.C.T., P.H., B.B., D.C., D.E.R., J.S.M., and D.C. Resources: M.G., H.K., J.S., B.C.T., and A.V.J. Data curation: B.B., J.S.M., P.H., D.C., M.G., B.C.T., and H.K. Writing—original draft: J.S.M. Writing—review and editing: J.S.M., A.V.J., J.S., M.G., B.C.T., B.B., P.H., D.E.R., and H.K. Visualization: J.S.M. Supervision: A.V.J., J.S.M., M.G., H.K., J.S., B.C.T., B.B., and P.H. Funding acquisition: J.S.M., A.V.J., M.G., H.K., J.S., B.C.T., B.B., and P.H. Project administration: J.S.M., A.V.J., M.G., H.K., J.S., B.C.T., and P.H. **Competing interests:** The authors declare that they

have no competing interests. **Data and materials availability:** The R code for all reported analyses is available on Github (https://github.com/Jordan-Scott-Martin/Tsimane-neighbor-IGEs) and Zenodo (doi: 10.5281/zenodo.15096836). Individual-level data are stored in the THLHP Data Repository and are available through restricted access for ethical reasons. THLHP's highest priority is the safeguarding of human subjects and minimization of risk to study participants. The THLHP adheres to the "CARE Principles for Indigenous Data Governance" (Collective Benefit, Authority to Control, Responsibility, and Ethics), which assure that the Tsimane (i) have sovereignty over how data are shared, (ii) are the primary gatekeepers determining ethical use, (iii) are actively engaged in the data generation, and (iv) derive benefit from data generated and shared for use whenever possible. The THLHP is also committed to the "FAIR Guiding Principles for scientific data management and stewardship" (Findable, Accessible, Interoperable, Reusable). Requests for individual-level data should take the form of an application that details the exact uses of the data and the research questions to be addressed, procedures that will be used for data security and individual privacy, potential benefits to the study communities, and procedures for assessing and minimizing stigmatizing interpretations of the research results (see the following webpage for links to the data sharing policy and data request forms: https://tsimane.anth.ucsb.edu/data.html). Requests for individual-level data will require institutional IRB approval (even if exempt) and will be reviewed by an Advisory Council composed of Tsimane community leaders, community members, Bolivian scientists, and the THLHP leadership. The study authors and the THLHP leadership are committed to open science and are available to assist interested investigators in preparing data access requests. All other data needed to evaluate the conclusions in the paper are present in the paper and/or the Supplementary Materials.

Submitted 7 August 2024
Accepted 2 July 2025
Published 30 July 2025
10.1126/sciadv.ads3129